REVIEW

Check for updates

Recent advances in flexible multifunctional electrochromic devices

Jiamin Yu,[a] Shanjie Wang,[a] Lin Gao,[b] Guoqi Qiao,[a] Meng-Fang Lin, [ID] [c]
Cong Wei, [ID] [a] Jingwei Chen [ID] *[d] and Shaohui Li [ID] *[a]

Electrochromism refers to the phenomenon in which certain materials undergo a redox reaction under an applied voltage or current, resulting in reversible changes in their optical properties and color appearance. Electrochromic devices (ECDs) show great potential in smart windows, anti-glare rear-view mirrors and displays due to the advantages of low energy consumption and simple control mechanisms. However, traditional ECDs are unfavorable for wearable and deformable optoelectronics due to the structural rigidity and limited functions. Thus, flexible ECDs integrating visual information with other advanced technologies can realize multifunctionality and further expand their application fields. This review first introduces the structure and recent development of flexible ECDs, followed by comprehensively summarizing the recent development of flexible multifunctional ECDs, including energy harvesting, energy storage, multicolor displays, and smart windows. Finally, the challenges, development trends and future prospects in flexible multifunctional ECDs are proposed and discussed. We hope that this review can guide and accelerate the development of flexible multifunctional ECDs in the new era of smart optoelectronics.

[a]School of Materials Science and Engineering, Zhengzhou University, Zhengzhou, 450001, P. R. China. E-mail: Shaohuili@zzu.edu.cn
[b]Hubei Key Laboratory of Energy Storage and Power Battery, School of Mathematics, Physics and Optoelectronic Engineering, Hubei University of Automotive Technology, Shiyan 442002, P. R. China
[c]Department of Materials Engineering, Ming Chi University of Technology, New Taipei City 24301, Taiwan
[d]School of Materials Science and Engineering, Ocean University of China, Qingdao 266100, P. R. China. E-mail: chenjingwei@ouc.edu.cn

1 Introduction

In nature, chameleons display different colors and patterns by controlling and regulating the activity of pigment cells on the skin.[1] In the physical world, chromism is the result of alterations in the various structural parameters of the material in response to heat, applied potential, light, solvent/vapor, *etc*.[2] To date, several types of chromism phenomenon have been

Jiamin Yu is currently a Master's student in the School of Materials Science and Engineering at Zhengzhou University, China. She is doing research under the supervision of Associate Professor Shaohui Li. Her current research focuses on multifunctional sodium/zinc-ion hybrid capacitors.

Jiamin Yu

Jingwei Chen joined the School of Materials Science and Engineering, Ocean University of China, as an associate professor in 2021. He obtained his Ph.D. from Nanyang Technological University (NTU) in 2019 under the supervision of Prof. Lee Pooi See, and did his postdoctoral research in NTU and the Singapore-HUJ Alliance for Research and Enterprise, Campus for Research Excellence and Technological Enterprise.

Jingwei Chen

His research focuses on the design, fabrication and mechanism understanding of novel electrode materials for electrochemical energy storage and energy saving devices, including metal-ion batteries and electrochromic devices.

discovered and studied, including thermochromism,[3] electro-chromism,[4] photochromism[5] and solvetochromism.[2] Among these, electrochromism refers to the phenomenon of reversible changes in optical properties (absorbance/transmittance/reflectance) of materials/devices through redox reactions under small applied voltages or currents, which are then macroscopically manifested as a change in the color of the material.[6–8]

In the early 1960s, Platt first proposed the concept of "electrochromism" and defined it as "a possible change of color producible in dyes by an electric field".[9] In the late 1960s, Deb first prepared ECDs using amorphous WO_3 films and proposed the theory of "oxygen vacancies color centers".[10] Up to the 1980s, the concept of "smart windows" initiated a new era of research on the application of electrochromic technology.[11] At this point, ECDs gradually began to form industrialized applications. In recent years, most of the ECDs are rigid due to the use of conductive glass substrates, which inevitably makes the devices rigid, bulky and heavy.[12,13] Therefore, the limitations of rigid ECDs limit the realization of a multitude of potential applications. To further expand the practical applications of ECDs, researchers have improved the flexibility of the devices in terms of substrate, electrolyte, and device structure to realize applications in the emerging field of wearable and deformable electronics.[14]

In addition, to further achieve the wide adoption of EC technology in the new era of the internet of things (IoT), researchers' interest has shifted in recent years to integrate EC technology with other advanced technologies to achieve multi-functionalities, which can promote and expand its potential applications.[15–17] For example, in order to address the issue of an external power supply to the device, EC systems are integrated with energy harvesting devices, including solar cells, nanogenerators, and galvanic cells, to realize self-powered ECDs, which can greatly improve the independence and portability of the ECDs. Due to the analogous structural features and reaction mechanisms of EC and electrochemical

materials, electrochromic energy storage devices (ECESDs) can also be designed to achieve both optical–thermal modulation and energy storage/release upon demand.[18,19] In particular, by choosing a suitable flexible substrate, the ECDs can be constructed into fabric or fiber-shaped devices, which can minimize the size and provide suitability for wearable or deformable electronic applications. Although these interests in EC systems have gained considerable attention and the relevant publications and citations are rapidly increasing with time,[18,20,21] a comprehensive and insightful summary on flexible multifunctional ECDs is still lacking. With the significant achievements made in transparent substrates, transparent conductors, EC materials, electrolytes, and device structures on flexible multifunctional ECDs, a timely and systematic summary is urgently needed.

Herein, in this review, we summarize and discuss the recent advances in flexible multifunctional ECDs, including flexible self-powered ECDs, flexible ESECDs, flexible multicolor displays, and flexible EC smart windows. In addition, the device configurations, design principles, integration mechanisms, material selection and performance optimization for flexible multifunctional ECDs are highlighted. Finally, the challenges and future development trends of flexible multifunctional ECDs are outlooked.

2 Configuration of flexible ECDs

As shown in Fig. 1, conventional ECDs have a sandwich symmetric structure, which includes a transparent substrate, transparent conductor, EC layer, electrolyte layer, ion storage layer, another transparent conductor, and a substrate layer.[18,22,23] The configuration of flexible ECDs is similar to that of rigid ECDs. The only difference between the two is that flexible ECDs use flexible and mechanically robust substrates to replace the "rigid" substrates. By infusing ECDs with mechanical properties such as flexibility, stretchability and deformability, various new high-end applications, such as adaptive camouflage, biomimicry, wearable displays, and color-changing cloth, can be achieved.[24] Although the structural differences between these two types of ECD are small, flexible ECDs still face numerous challenges that need to be overcome, including poor substrate flexibility, performance degradation, accompanying deformation, and electrolyte leakage during mechanical strain/stress processes.[25] In addition to the conventional ECDs, which focus on ion intercalation/deintercalation as shown in Fig. 1, reversible metal electrodeposition-type electrochromic devices (RMEECDs) have also been widely explored in recent years.[18] RMEECDs, which are based on reversible electrodeposition and dissolution of metals, have a simpler layer structure and a wider range of optical states (transparent, colored and mirrored states).[26,27]

2.1 Soft/flexible substrate

The substrate is the outermost layer of the ECDs and mainly plays the role of supporting the whole device to ensure a high

Shaohui Li received his Ph.D. degree in 2015 from the Huazhong University of Science and Technology, China. Then, he worked as a postdoctoral researcher at Nanyang Technological University. In 2019, he joined the School of Materials Science and Engineering, Zhengzhou University of China, as an associate professor. His main research interests focus on the design, fabrication and mechanism understanding of novel electrode materials for electrochemical energy storage and energy saving devices, including lithium/sodium/zinc-ion capacitors and electrochromic devices.
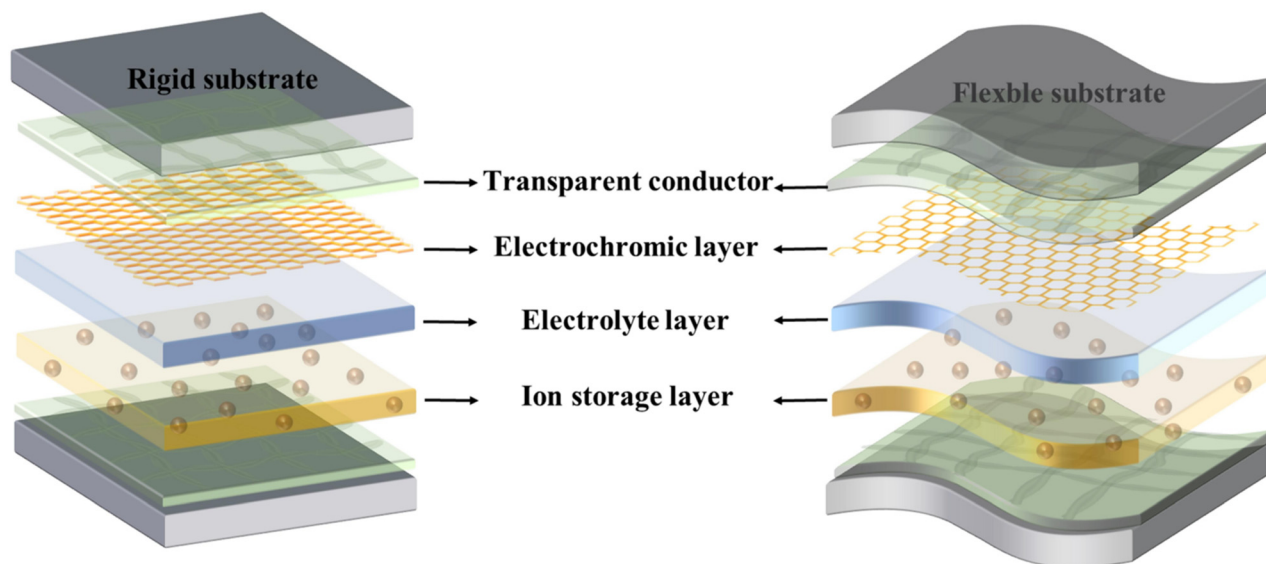
Shaohui Li

Fig. 1 Device configuration comparison of rigid and flexible ECDs.

mechanical strength. Compared with rigid substrates, flexible substrates offer the advantages of flexibility, light weight and low cost, ease of handling, and suitability for mass production, which allows flexible ECDs to maintain their EC performance under bending, stretching, or twisting, and expands the range of applications.[28,29] Common flexible substrate materials include poly(ethylene) (PE), polyethyleneimine (PEI), polyimide (PI), polyethylene naphthalate (PEN), poly(ethylene terephthalate) (PET), and poly(dimethylsiloxane) (PDMS).[30–35] Among these substrates, PET is the most widely reported substrate due to its colorlessness, chemical inertness, and excellent mechanical properties. Especially, PET also displays excellent thermal stability, which allows the facile preparation of PET-based transparent conductors under mild temperatures.[25] Unfortunately, PET is non-biodegradable in nature, which easily causes environmental pollution problems. In recent years, researchers have identified and demonstrated the advantages of nanocellulose over commonly used plastic substrates due to its high mechanical strength, tunable optical transmittance, renewability, biodegradability and environmental friendliness.[33,36,37] The fabricated ECDs also exhibit excellent flexibility, bendability and even foldability. However, to date, there is still a lack of an efficient way to fabricate transparent nanocellulose substrates on a grid-scale, which further limits the widespread application in EC systems.

2.2 Transparent conductor

The transparent conductor as the connection between the device and the external power supply can reduce the electron transfer resistance and enhance the charge transfer, which is required to have the advantages of good light transmittance, low resistivity, and good electrochemical stability.[23,24] Indium tin oxide (ITO) and fluorine-doped tin oxide (FTO) are the most commonly used transparent conductors in conventional

ECD manufacturing due to their superior optical and electrical properties. The ITO or FTO layers are usually deposited on ultrathin silica-boron glass using vacuum evaporation, magnetron sputtering, chemical vapor deposition (CVD), or sol–gel methods.[38] In order to satisfy application in flexible electronics, ITO can also be deposited on a PET or PEN substrate instead of rigid glass and this has been commercialized in the market.[39] For example, Li *et al.*[40] deposited $W_{18}O_{49}$ nanowires on a commercial ITO/PET transparent conductor as an EC electrode, and the fabricated ECDs display good mechanical flexibility. However, the inherent brittleness and poor adhesion of ITO makes it unfavorable in flexible and deformable ECDs, thus necessitating the development of more suitable flexible transparent conductors.[41] In recent years, a variety of flexible transparent conductors have been investigated, including conducting polymers,[42,43] carbon nanotubes (CNTs),[44,45] graphene,[46,47] MXene,[48,49] metal nanowires,[50] and metal grids,[51] which can replace the traditional ITO/FTO and greatly promote the development of flexible ECDs. For example, Cai *et al.*[52] prepared a stretchable transmission ECD by inkjet printing WO_3 nanoparticles on an elastomeric transparent conductor based on silver nanowires (AgNWs). The device displayed excellent EC performance and can be stretched up to 50%, showing promise for wearable and deformable electronics.

2.3 EC layer

The EC layer is the fundamental component for the flexible ECDs, and can change color under the action of an electric field. The EC layer is composed of EC materials and great efforts have been devoted to designing different EC materials during the past decades. Currently, the EC materials can be divided into inorganic materials (*e.g.*, WO_3,[53,54] MoO_3,[55] TiO_2,[56,57] NiO,[58,59] MnO_2,[60] V_2O_5[61,62]), organic materials (*e.g.*,

polyaniline (PANI),[63] polypyrrole (PPy),[64] poly(3,4-ethylenedioxythiophene):poly(styrenesulfonate) (PEDOT:PSS),[65] viologen[66]), and inorganic–organic hybrid materials[20,21] (*e.g.*, $Ni(OH)_2$/PEDOT, PANI/$WO_{2.7}$, MoO_{3-x}@PANI, WO_3/PEDOT:PSS).[67–69] Inorganic materials usually have the advantages of good stability, high reliability and a wide operating temperature range, but suffer from monotonous colors, slow switching speed and high manufacturing costs.[70,71] In contrast, organic materials can offer fast response times, rich colors, high processability, light weight, and natural flexibility, which makes them very suitable for fabricated flexible ECDs, but they usually have inferior heat resistance, durability, and chemical stability.[72–74] Recently, coupling inorganic and organic materials together to construct flexible ECDs has attracted growing interest due to the synergistic effect. For instance, E. Eren *et al.*[69] prepared a PANI and WO_3 composite EC electrode and fabricated a flexible ECD, exhibiting a large optical modulation (38.7%), rapid coloration time (6.4 s), and excellent mechanical stability (only 7.5% optical contrast degradation after 100 bending cycles). The development of EC composite materials has shown great potential and may open new possibilities for flexible ECDs.

2.4 Electrolyte layer and ion storage layer

The electrolyte layer, also known as the ion conductive layer, supplies the compensation ions required by the EC material and prevents short circuits between the two electrodes.[75] The ionic conductivity and temperature tolerance of the electrolyte can directly affect the performance of ECDs, including switching time, durability, and operating temperature range. The electrolyte can be classified into three categories based on its physical state: liquid, solid, and gel (semi-solid).[76] In addition, the electrolyte must have suitable ion conductivity, good optical transmission, high thermal stability, and safety.[77]

The ion storage layer, also known as the counter-electrode layer, serves the function of maintaining the charge balance and ion storage during electrochemical reactions, exemplified by NiO and TiO_2.[22] In addition, to enhance the optical modulation and coloration efficiency (CE) of ECDs, a complementary EC layer can also be used as an ion storage layer and exhibited a color change when the devices are colored. For the multivalent ion-based ECDs, the metal anodes can directly work as the ion storage layer *via* reversible metal plating/stripping kinetics.[78] Taking the new type of zinc-based ECDs as an example, the zinc plays the role of a counter-electrode to balance the charge.

3 Recent progress of flexible multifunctional ECDs

3.1 Self-powered flexible multifunctional ECDs

Although ECDs have the advantages of a low driving voltage and small current, they still need an external energy supply to achieve the chromism function, which significantly affects the independence and portability of ECDs.[79,80] To address these problems, the concept of self-powered ECDs is proposed based on the integration of ECDs and energy harvesting technology. This integrated technology enables the ECDs to obtain the necessary energy (*e.g.*, solar, mechanical, chemical) from its operating environment and convert it into electrical energy, driving the ECDs to realize the color-changing function.

3.1.1 Solar-driven flexible multifunctional ECDs. Solar-driven self-powered flexible multifunctional ECDs convert solar energy into usable electrical energy, to drive ECDs to achieve a color change, thus forming self-powered photoelectrochromic devices (PECDs).[20] Currently, there are two main types of integrated structure for PECDs, namely the juxtaposing type with two independent devices in combination and a single-handed type in a single device. In the juxtaposing-type PECDs, the ECDs and the photovoltaic cell are connected in series. For example, Davy *et al.*[81] integrated a dual-band ECD with near-ultraviolet solar cells together, where the solar cell can generate an open-circuit voltage of more than 1.6 V and drive smart windows to modulate visible and near-infrared light by selectively collecting near-ultraviolet photons. However, the juxtaposing-type PECDs suffer from the problems of inconvenient circuit connection, complex structure, heavy mass and large volume, which make it difficult to construct flexible devices. In contrast, the single-handed type usually integrates a photovoltaic device electrode and an EC layer into a single device, which can greatly simplify the structure and reduce the weight of the device.[20] For example, Cánovas-Saura *et al.*[82] fabricated a fully large-area (900 cm^2) printed flexible PECD using PEDOT-PSS as the EC layer, and V_2O_5 as the transparent ion storage counter-electrode, and realized self-regulation by using organic solar modules. The PECD displays a 25% contrast at 650 nm and a fast switching speed less than 30 s. Similarly, Zhang *et al.*[83] reported a smart and self-powered flexible EC window with self-regulating functions and high stability. The flexible PECD can adjust the transmittance in real time with the change of sunlight intensity. As shown in Fig. 2a, the system is composed of Ag@Au core–shell nanowires, an ethyl viologen and a commercial solar cell as flexible transparent electrodes, chromophore and power source, respectively. The transmittance gradually decreases when the sunlight intensity increases, while the window transforms into a bleached state when the sunlight intensity increases (Fig. 2b and c). The as-fabricated flexible PECDs (Fig. 2d and e) show a high optical contrast (41% at 605 nm), superior CE (106 cm^2 C^{-1}), and excellent cycling stability (20% optical contrast degradation after 4000 cycles).

3.1.2 Nanogenerator-driven flexible ECDs. Compared with solar energy, mechanical energy, which is available and independent of external weather and other factors, has attracted a lot of attention to convert low-frequency mechanical energy into electrical energy, which can be used to power ECDs. In particular, nanogenerators can also convert the mechanical energy of human motion into electrical energy at the nanoscale, which can be used to power wearable electronics.[84] For instance, He *et al.*[84] fabricated a piezoelectric-driven self-powered patterned EC supercapacitor. The piezoelectric nanogenerator (PENG) was prepared by electrospinning polyvinyli-
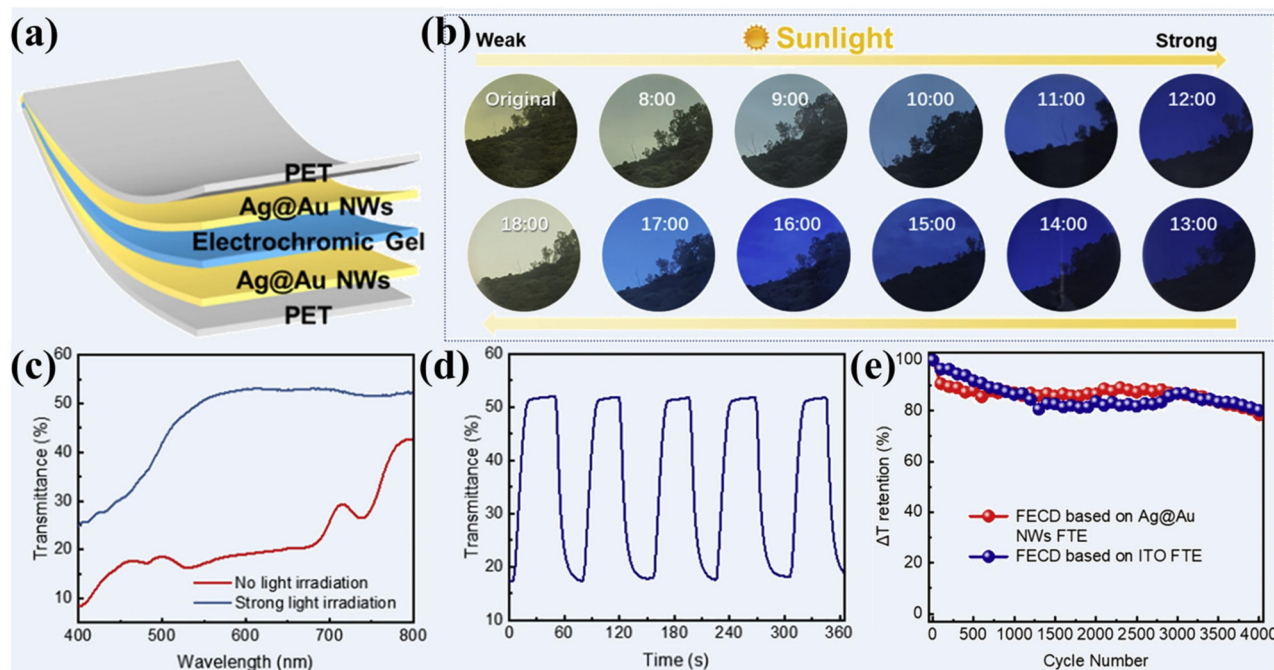
Fig. 2 (a) Schematic illustration of the PECD; (b–e) characterization of a self-powered EC system based on Ag@Au NWs. Reproduced with permission.[80] Copyright 2022 Elsevier.

dene difluoride (PVDF) thin films and the visual EC part was constructed by an electrodeposition-patterned PANI electrode. Due to the flexibility and biocompatibility of the PVDF and PANI, the self-powered ECDs can be attached to the human body to harvest the human motion energy and store it in the ECDs. The whole system can be used as a visual sustainable energy source to power wearable electronics without an external energy supply. Similarly, Bi et al.[85] demonstrated a flexible PENG-driven tactile display by constructing a PVDF-based pressure sensor and PANI-based ECD. When applying different voltages, the ECD can show four colors of light yellow, green, blue and dark blue (Fig. 3a and b). Thus, the system can directly monitor the motion trajectory and pressure intensity from the color change of the ECD. Recently, a tandem self-powered ECD system was developed by Huang et al.[86] The system integrates the triboelectric nanogenerators (TENGs), organic photovoltaics, and EC supercapacitor together, thus enabling the device to harvest and store the energy from both light and human motion, demonstrating all-day operation application. Benefiting from the intrinsic integration, the tandem device exhibits superior flexibility and durability with a reduced thickness of 52% and improved power-per-weight of 110%. This progress clearly shows the potential application of nanogenerator-driven flexible ECDs, but their practical applications are still limited by the slow color switching speed and low optical contrast due to the limitations of low output power and the complex structure of PENGs and TENGs.[87]

3.1.3 Chemistry-driven flexible ECDs. Chemical energy-driven ECDs are usually the fusion of the galvanic cell and ECD together with an active metal anode and an EC cathode,

which can directly convert chemical energy into electrical energy and drive the color change.[88] Compared with the above two self-powered flexible ECD systems, chemical energy-driven ECDs have two advantages: (1) the introduction of active metal electrodes simplifies the structure of ECDs and significantly reduces the energy consumption; and (2) they can be used as a visual rechargeable battery and monitor the energy storage state through the color changes.[89] Wang et al. demonstrated a self-powered flexible ECD by fusing an Ag/$W_{18}O_{49}$ nanowire film and Al sheet in a single cell, as shown in Fig. 3c and d.[90] The self-powered flexible ECD can provide an open-circuit voltage of 0.83 V due to the potential difference between two electrodes, which is sufficient to drive the coloration of the $W_{18}O_{49}$ nanowires. The device can color in 14 s with an optical contrast of 40% after connecting the EC electrode and Al sheet. Meanwhile, the device can bleach after 700 s with the two electrodes disconnected. In addition, the self-powered flexible ECD can be easily scaled up to 20 × 20 cm, which shows great practical applications in flexible ECDs. Similarly, the metals Zn and Mg can also be applied as an active anode to fabricate chemistry-driven flexible ECDs, and especially for the metal Mg, the self-powered system exhibits a large optical contrast and fast response time due to the larger potential difference (−2.37 V vs. standard hydrogen electrode).[91–93] However, the use of Zn or other metal as active anode will lead to several issues, including an internal short circuit, interfacial corrosion, and dendritic formation, which will result in unfavourable cycling stability for the ECDs.[94] Currently, many strategies, including alloy coating,[95] surface modification,[96] and Zn matrix engineering,[97] have shown that these issues can be
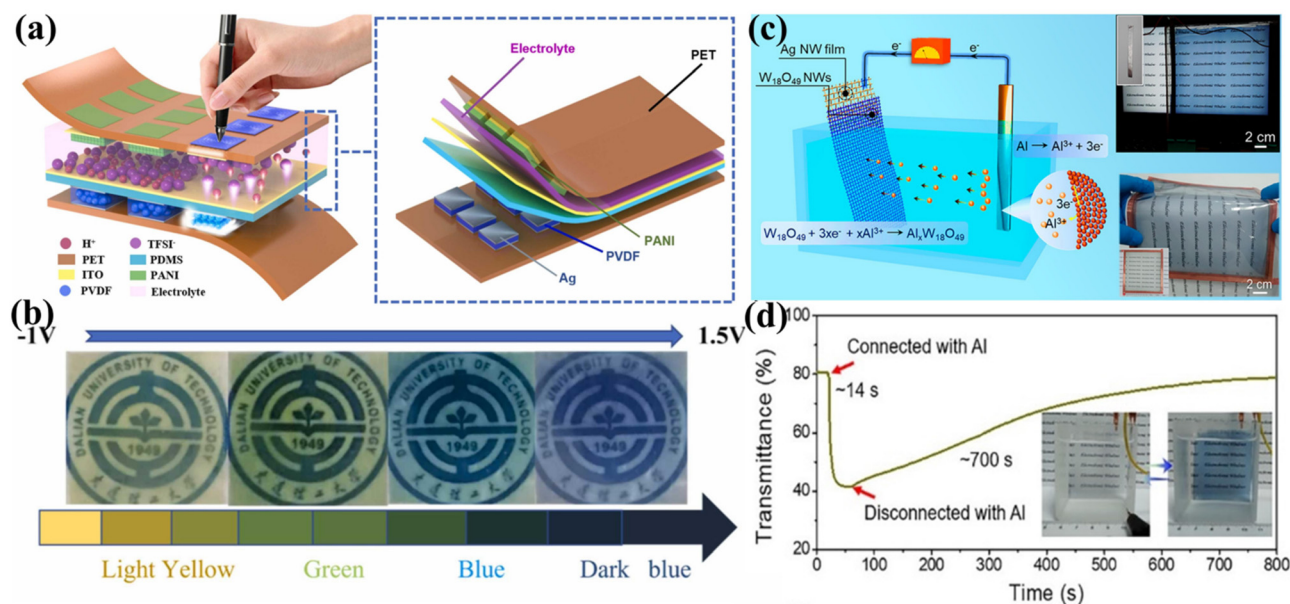
Fig. 3 (a) Schematic illustration of the PENG-driven tactile display; (b) the color variance under different applied voltages. Reproduced with permission.[82] Copyright 2022 Elsevier Ltd. (c and d) Schematic illustration and characterization of the self-powered flexible EC galvanic cell. Reproduced with permission.[85] Copyright 2021 American Chemical Society.

effectively mitigated in Zn ion batteries, which could also solve the problems in metal active anode-based ECDs.

3.2 Flexible electrochromic energy storage

Energy storage devices (ESDs) mainly include supercapacitors and batteries.[98] Importantly, ECDs share similar characteristics to ESDs in terms of material type, device configuration, and reaction mechanism. Therefore, it is possible to achieve a multifunctional integration of an EC and energy storage device in a single cell, which allows for both energy recovery in the process of color change and monitoring the level of stored energy in the device through the color change.[20,99] In EC energy storage devices (ECESDs), advanced flexible devices possess better functionality than traditional rigid glass-based devices and can be integrated with a curved surface, showing potential applications in smart windows, smart wearables, low-energy electronics, and renewable energy sources.[100] However, in flexible ECESDs, dissociation, degradation, and delamination occur at the electrodes/electrolytes interface, which seriously affect their performance, and become key issues that need to be solved before commercialization.[21] In this section, we summarize the recent progress on flexible EC supercapacitors (ECSCs) and flexible EC batteries (ECBs).

3.2.1 Flexible electrochromic supercapacitors. Supercapacitors (SCs) are one of the most widely investigated energy storage devices due to their high safety, superior power density, and long operating lifespan.[21,101–103] Recently, with the development of IoT and the growing demands of wearable electronics, the ECSCs have garnered significant attention due to their ability to simultaneously provide energy storage and color transition. For example, WO_3 is a typical ECSC material due to its EC properties and pseudocapacitive behavior

through the cation insertion/extraction, accompanied by a reversible redox reaction of $W^{6+}/W^{5+}/W^{4+}$.[104,105] The first WO_3-based flexible ECSC was reported by Shen et al.[106] in 2016, where the electrode was constructed by using a AgNW/WO_3 hybrid film. Owing to the reversible H^+ intercalation/deintercalation on the electrode, the color can be reversibly changed between colorless (55.9% at 633 nm) and dark blue (11.8% at 633 nm). The as-made ECSC demonstrates an excellent electrochemical performance of 138.2 F g^{-1} at 10 mV s^{-1} with a high CE of 80.2 cm^2 C^{-1} (Fig. 4a–c). In order to solve the electrochemical stability of AgNWs and the delamination issue between AgNWs and the substrate, Hao et al.[107] designed a flexible WO_3@AgNW PDMS electrode by embedding the core–shell structured WO_3@AgNW into a PDMS substrate. The architecture of the electrode can solve the delamination problem during bending tests and the core–shell structure of WO_3@AgNW can inhibit the oxidation of AgNWs and improve the electrochemical stability. The WO_3@AgNW-PDMS electrode demonstrated remarkable electrical conductivity stability ($\Delta R/R = 8.3\%$) and EC performance (90% optical modulation retention) after 20 000 bending cycles. Similarly, Zhang et al.[108] coat the AgNW micromesh with a thin Au layer. Cai et al.[109] protected the Ag grid/PET transparent conductor with a PEDOT:PSS layer. These strategies greatly improve the chemical stability of the Ag-based transparent conductor in acidic and alkaline conditions with robust mechanical stability. However, the poor electronic conductivity and limited specific capacity of WO_3 hinder its further applications in ECSCs and in energy-saving fields. As an alternative, Hassan et al.[110] prepared a multilayer flexible ECSC electrode by depositing $W_{18}O_{49}$ NW/$Ti_3C_2T_x$ composite onto a pre-assembled Ag and $W_{18}O_{49}$ NW-based transparent conductive network. The
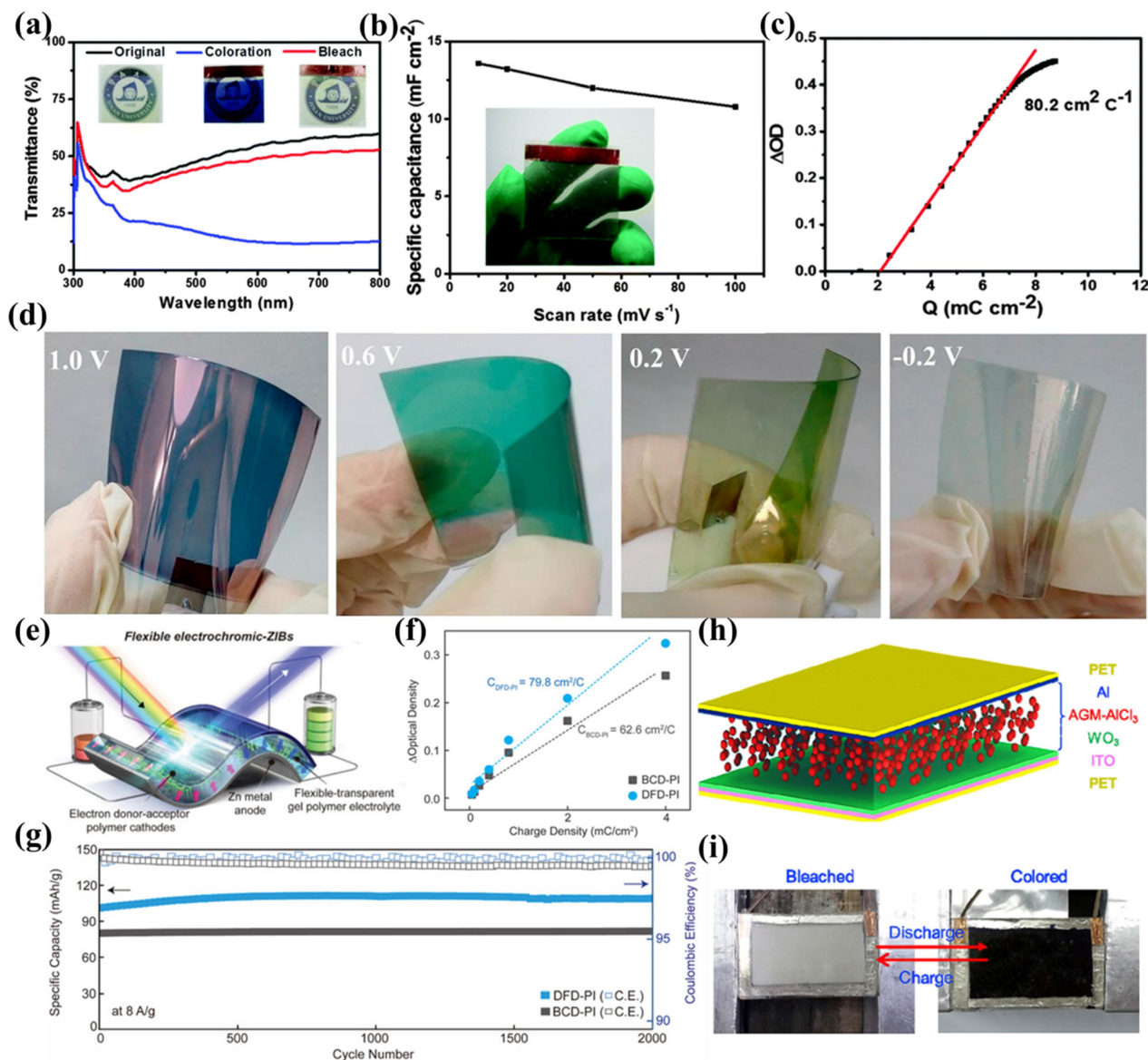
Fig. 4 (a) Transmittance spectra of the Ag NW/WO$_3$ electrode; (b) areal capacitance as a function of scan rate (the digital images of the flexible ECSC electrode); (c) optical density *versus* charge density of the Ag NW/WO$_3$ electrode. Reproduced with permission.[99] Copyright 2016 Royal Society of Chemistry. (d) The colored state of the flexible PANI film at the different potentials. Reproduced with permission.[107] Copyright 2018 Elsevier B.V. (e) Schematic of flexible electrochromic–ZIBs; (f) the average CE of BCD-PI and DFD-PI; (g) cycling performance at a current density of 8 A g^{-1}. Reproduced with permission.[117] Copyright 2023 Wiley-VCH GmbH. (h) Schematic of the structure of a flexible ECB. (i) Photos of ECB in bleached and colored states. Reproduced with permission.[118] Copyright 2020 Elsevier B.V.

obtained electrode can display a high areal capacitance of 125 mF cm^{-2} and remarkable optical modulation of 98.2%. The as-constructed bifunctional symmetric ECSC device delivered excellent SC properties (energy density of 10.26 μW h cm^{-2} and power density of 0.6 mW cm^{-2}) and EC performance (fast switching time of 5/7 s (coloring/bleaching) and high CE of 116 cm^2 C^{-1}). Similarly, MoO$_3$,[111] V$_2$O$_5$,[112] Nb$_2$O$_5$,[113] Nb$_{18}$W$_{16}$O$_{93}$,[114] and NiO[115] *etc.* have also been investigated for the design of flexible ECSCs and great progress has been made, which significantly promotes the development of flexible ECSCs.

Due to the instinctive brittleness of metal oxides, the EC and energy storage performance of the fabricated flexible ECESDs were easily degraded by the cracks formed during the repeated bending process.[116] In contrast, organic materials have the merits of flexibility, lightness, and compatibility, which find various applications in optoelectronics. For example, Zhang *et al.*[117] prepared a flexible nanoporous 3D conjugated polymer network-based ECSC electrode by electro-polymerizing triphenylamine (TPA) and 3,4-ethylenedioxythio-phene (EDOT). The resulting electrode displayed a high specific capacitance (137 F g^{-1}, 1 A g^{-1}), excellent cycling stabi-

lity (91.1% capacitance retention after 6000 cycles), and reliable EC behavior (optical modulation of 33% and coloration efficiency of 136 cm^2 C^{-1} at 450 nm). The assembled flexible ECSC device also demonstrated excellent mechanical stability and EC performance with a multicolor change from blue-green to violet, manifesting the visual monitoring of energy storage. Similarly, Zhou et al.[116] prepared a flexible PANI-based ECSC film on an ITO/PET substrate by galvanostatic and cyclic voltammetric electrodeposition. The obtained PANI electrode showed a reversible multicolor change between transparent, pale yellow, green, blue and blue-purple (Fig. 4d), a high coloration efficiency of 80.9 cm^2 C^{-1} at 630 nm and highest specific capacitance of 473.3 F g^{-1} at a scan rate of 30 mV s^{-1}, demonstrating its promising applications in flexible and multicolor electronics and optoelectronic devices.

3.2.2 **Flexible electrochromic batteries.** Compared with SCs, batteries usually can store more energy due to a slow diffusion-limited Faraday reaction, needing a longer time to finish the charge/discharge process.[64] Despite the limitations, research on ECBs has grown rapidly in recently years due to the high energy density that can supply more power for wearable and smart electronics.[118–120] Multivalent ion-based ECBs, including Zn^{2+},[121,122] Al^{3+},[123,124] and Ca^{2+},[125] have become a research spotlight due to the higher charge density, higher energy density, and metal anode serving as ion-storage layers from the reversible switch between metal and metal cations. The first flexible ECB was prepared by Wang et al.,[64] and the device was constructed by an electrodeposited PPy as the cathode and an electrodeposited Zn as anode. The fabricated Zn//PPy battery can deliver a high capacity of 123 mA h g^{-1} with a color change from black to yellow when the voltage changes from 1.2 to 0 V. Similarly, Ding et al.[126] prepared a flexible Zn/Prussian blue (PB) battery-type ECD by directly depositing PB film on the ITO/PET substrate as EC cathode and Zn sheet as anode. The produced device exhibited an excellent EC performance with an optical contrast of 68.3% at 700 nm, high CE of 117.2 cm^2 C^{-1}, and fast switching time of 4.7/7.5 s (coloration/bleaching). In addition, the device also displayed superior energy storage properties with a large areal capacity of 77.1 mA h m^{-2}, high output voltage of 1.4 V, and remarkable cycling stability maintaining 78% of the initial optical modulation after 1000 cycles. Yun et al.[127] reported a flexible zinc-based ECB by employing a "π-bridge spacer"-embedded electron donor–acceptor polymer as cathode. The π-bridge spacer can alternate the electron donor and electron acceptor in the polymeric skeleton, which can significantly improve the ion/electron migration, endowing the flexible ECB with a high specific capacity of 110 mA h g^{-1} at a current of 8 A g^{-1} and a large CE of 79.8 cm^2 C^{-1} under severe mechanical deformation (Fig. 4e–g). In order to further improve the specific capacity of ECB, Sun et al.[128] prepared a flexible and rechargeable aluminum-ion ECB by using WO$_3$ film, Al, PET/ITO and aluminum trichloride (AlCl$_3$) aqueous solution as cathode, anode, substrate and electrolyte, respectively. Owing to the smaller ionic radius of Al^{3+} than Zn^{2+}, the assembled ECB can deliver a high specific capacity of 142 mA h g^{-1} and

reversible color transition between white and dark blue (Fig. 4h and i). Although great progress has been made in flexible ECBs in recent years, the fabrication of the flexible ECBs is still limited by the opaque and rigid metal-based anode, which further induces irregular color contrasts and a long switching time due to nonuniform cation gradient distributions. To solve this limitation, Singh et al.[129] constructed a flexible Zn-based ECB by using a flexible and transparent Zn-nanofiber network as anode. By combining a PANI-based cathode, the fabricated flexible ECB can deliver a high optical contrast of 50%, large areal capacity of 174.8 mA h m^{-2}, and high volumetric energy density of 378.8 W h m^{-3} at a power of 562.7 W m^{-3}. In addition, the ECB also displays a reversible color transition between transparent and dark bluish-violet. Cai et al.[130] demonstrated a large area (810 cm^2) ECB film by electrospraying Fe(II)-based metallo-supramolecular polymer on an ITO/PET substrate, and the obtained EC films exhibited an ultrahigh coloration efficiency (750.3 cm^2) and fast switching speed (<1 s). These results manifest that the proposed flexible ECB is a promising pathway to develop ECBs for smart and flexible electronics applications.

3.3 Flexible multicolor displays

Multicolor ECDs (M-ECDs) are devices that are able to change between multiple colors based on the redox reaction of EC materials by adjusting their transmittance/reflectance in the visible light range.[131] Compared with mature display technologies that have been commercialized, such as liquid crystal displays (LCD) and organic light-emitting diodes (OLED), M-ECDs have the advantages of high transparency, high energy efficiency, high contrast ratio, low energy consumption, fast response time, easy observation, optical memory effect, and eye-friendliness.[74,80,132] Most of the current EC materials have good compatibility with a wide range of substrates, including glass, PET, fibers, and so on.[80] These advantages enable applications in smart windows, displays, and flexible and wearable electronics.[131] Generally, the M-ECDs can be classified into three categories: intrinsic chemical multicolored EC materials, color overlays from special architecture designs, and photonic crystal structure induced multicolors.

3.3.1 **Intrinsic chemical multicolor.** Due to the relatively fixed electronic energy band, most single-component transition metal oxides can only present a single color, such as WO$_3$, TiO$_2$, MoO$_3$, and NiO,[133] and thus, most reported ECDs are mainly focused on displaying a single color change or are construction patterned ECDs with one image demonstration. However, with the development of electronic papers/billboards and multimedia, the single-color ECDs cannot meet the needs, and the attention on multicolor ECDs has grown rapidly in recent years.[134] Owing to the multiple valence states of vanadium, V$_2$O$_5$ has a triple energy-band electronic structure, enabling a reversible color change between yellow, green, and blue when different voltages are applied, and these have become the most reported EC materials for M-ECDs.[135] Wu et al.[136] prepared a flexible multicolor EC film on a graphene/PET-based transparent conductor by electrochemical depo-

sition of V_2O_5. The deposited film exhibits a layered structure with an amorphous nature, which can facilitate the electrolyte penetration and reduce the ion diffusion barrier. The obtained multicolor EC film displays a superior CE of 555.8 cm^2 C^{-1} and ultrahigh transmittance modulation of 68.9% at 800 nm. Sun *et al.*[137] prepared V_2O_5-cellulose composite films by the spin-coating method and successfully assembled a flexible reflective ECD. Due to the valence state change of vanadium ions induced by the insertion/extraction of Li$^+$ and electrons, the device can deliver a reversible color transformation. As shown in Fig. 5a–c, the fabricated flexible M-ECDs can reversi-

bly work at a low drive voltage (−1 to 1 V) with a rapid switching speed (≤5.6 s) between the colors of yellow and blue. In addition, the M-ECDs also exhibit excellent cycling stability with less reflectivity lost after 1000 cycles. The novel device is able to provide a broad range of color modulations to simulate natural conditions, enabling potential applications in forests, grasslands, or deserts. Furthermore, the flexible M-ECDs are also compounded with energy storage and energy harvesting to achieve more functional integrated device applications. Liu *et al.*[138] assembled a flexible zinc ion electrochromic battery (ZIEB) using a sodium vanadate cathode, ion redistributed
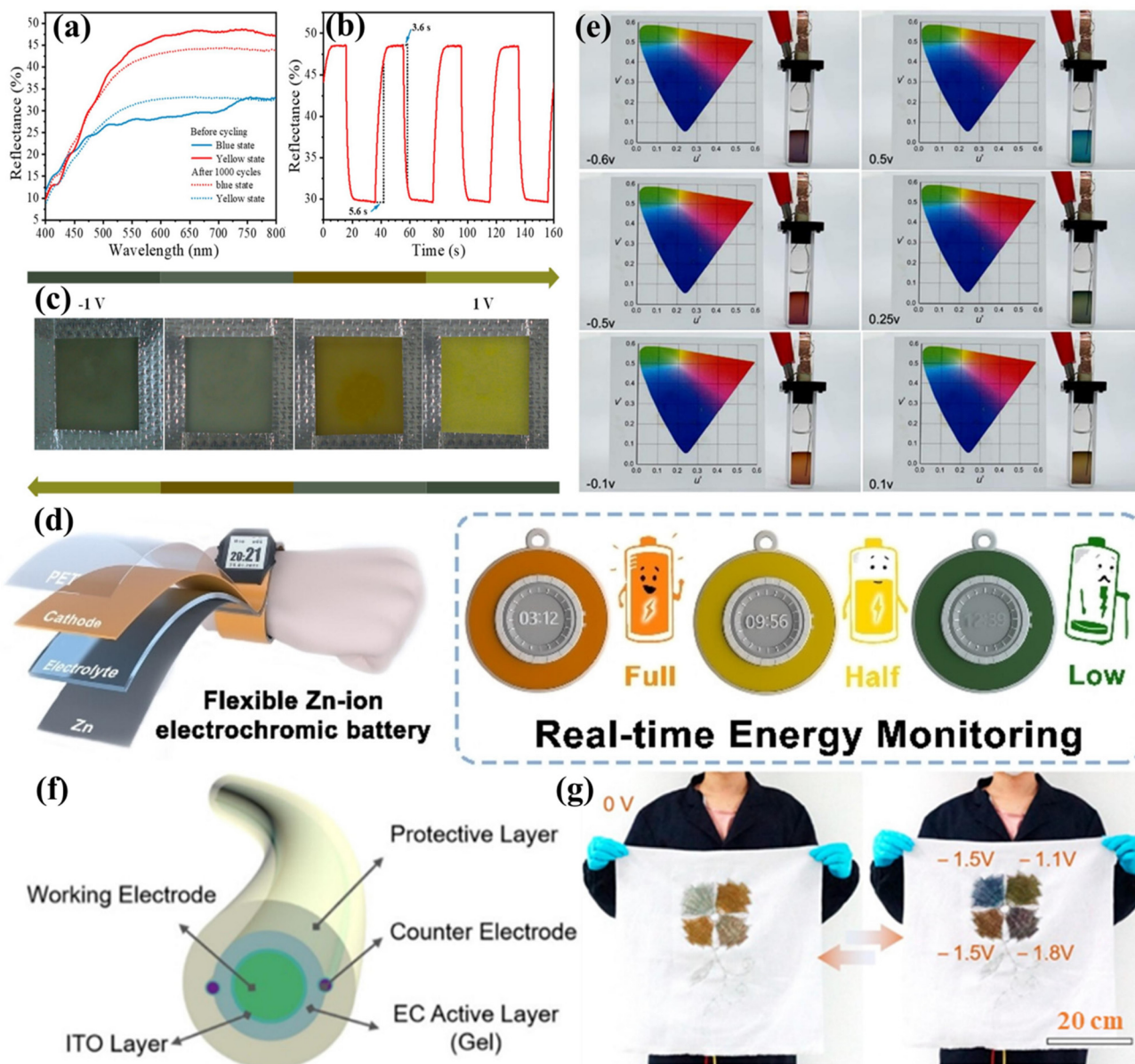

Fig. 5 (a) Reflectivity changes of the device in different states; (b) *in situ* reflectance change of the device; (c) device color modulation window. Reproduced with permission.[126] Copyright 2022 American Chemical Society. (d) Illustration of a flexible ZIEB. Reproduced with permission.[127] Copyright 2024 Wiley-VCH GmbH. (e) Photographs of poly(PEP) film with an applied voltage from −0.6 V to 0.5 V. Reproduced with permission.[129] Copyright 2020 Elsevier B.V. (f) Structural images of the EC fibers; (g) digital photographs of the EC textile for large-area embroidery. Reproduced with permission.[130] Copyright 2020 American Chemical Society.

hydrogel electrolyte, and zinc anode to achieve the integration of energy storage and multi-color flexible electrochromic devices. As shown in Fig. 5d, the ZIEB has a continuous reversible color change from orange to brown and green and maintains a stable energy output after mechanical deformation.

As well as transition metal oxides, organic EC materials have also been employed for M-ECDs due to their lack of expense, rich colors, faster response speed, and easy preparation. As a typical organic EC material, PANI can reversibly switch the color between green, yellow and blue. For example, Huang et al.[139] reported PANI-based flexible and patterned ECDs by an inkjet-printing method. The ink was formulated with two-dimensional (2D) PANI in formic acid, which combines the nanoscale thickness and appropriate doping ratio, endowing the printed PANI electrodes with an excellent EC performance. The as-made EC electrode displays a high optical contrast (76% at 750 nm), fast coloration/bleaching response time (1.8/2.4 s), and superior CE (259.1 cm^2 C^{-1}). However, this color change still cannot meet the demand for a full spectral range of multicolor flexible ECDs. To solve this problem, Zhang et al.[140] reported an EC polymer based on 5,7-bis (3,3-dimethyl-3,4-dihydro-2H-thieno[3,4-b][1,4]dioxepin-6-yl)-2,3-dihydrothieno[3,4-b][1,4]dioxine (PEP). PEP combines several distinct polymers, and can reversibly tune a multicolor range. When the applied potential was gradually increased from −0.6 V to 0.5 V, the polymer can change color between purple, red, orange, yellow-green, green and blue (Fig. 5e). Unfortunately, typical organic EC materials can only switch from the natural color to the oxidized transparent state. Therefore, it is extremely complex to realize a multicolor range by compositing several different organic EC materials.

Furthermore, apart from the planar flexible M-ECDs, fiber-shaped or fabric-shaped M-ECDs are also a research hotspot and have developed rapidly in recent years due to the potential applications in wearable, smart display, military camouflage, and anti-counterfeiting technologies. Recently, a continuous, hundreds of meters long EC fiber suitable for industrial weaving was developed by Fan et al.[141] By introducing different EC materials and structural designs, multicolor changes can be achieved, including blue, magenta, green, and dull red. After introducing an outer polymer protective layer and electrochemical anticorrosive layer, the electrochemical, mechanical, washing, and thermal stabilities of as-produced fiber-shaped M-ECDs were greatly improved, making them wearable over large areas and implantable into smart color-changing textiles with complex patterns (Fig. 5f and g). Gao et al.[142] constructed M-EC fabrics by using PET fabric, PEDOT:PSS/dimethyl sulfoxide (DMSO), and ionic liquid as the substrate, conductive EC layer and electrolyte, respectively. The M-EC fabrics display excellent EC behavior with reversible color variations between light blue and dark blue. After coating with commercial hydrophobic agents, the M-EC fabrics can exhibit impressive hydrophobicity and self-cleaning properties, showing potential applications in adaptive camouflage and wearable displays.

3.3.2 Color overlay. As discussed above, the intrinsic multicolor EC materials are very limited, which significantly restricts the development of ECDs in multicolor display applications in the visible spectrum. To increase the color range of ECDs, according to color overlay principles, combining more than two EC materials together or using colorable electrolytes is thought to be an effective method. For instance, Ding et al.[143] prepared a flexible inorganic multicolor display by electrodeposition of MnO_2 and PB thin films as complementary electrodes. Owing to the color overlay, the constructed M-ECDs can achieve apparent changes to different degrees of yellow, green, and blue (Fig. 6a). The M-ECDs displayed a fast color response of 0.5 s, excellent CE of 144.2 cm^2 C^{-1}, and wide optical modulation of 40% at 710 nm. They also assembled a flexible quasi-solid M-ECDs by using a sputtering-made WO_3 anode and Prussian white@MnO_2 cathode (Fig. 6b).[144] The device delivered a high CE of 77.6 cm^2 C^{-1}, wide optical modulation of 35% at 510 nm, and excellent cycling stability without obvious degradation after 10 000 cyclic voltammetry cycles at a wide working voltage from −2 to 2.5 V (Fig. 6c–e). Xue et al.[145] proposed a flexible M-ECD by sandwiching an ionic gel electrolyte between two cathodic nickel hexacyanoferrate (NiHCF) and PB EC layers. Owing to the color overlay effect by two EC electrodes, the device displays four colors of green, blue, yellow and colorless. When introducing an Al wire as the anode, the device can be formed into a self-powered flexible M-ECD system, which can change color without an external power supply. Similarly, Zhang et al.[146] also demonstrated a self-powered M-ECD system by sandwiching a zinc anode between sodium vanadium oxide (SVO) and WO_3 electrodes, which exhibited a full color tunability and displayed 16 different colors, showing great practical application of Zn anode-based M-ECDs.

In addition to constructing M-ECDs by a multilayered structure of different EC materials, introducing functional ionic gel electrolytes by coupling redox-active species (e.g., electrochemiluminescent (ECL) luminophores, EC dyes) instead of conventional electrolytes is also thought to be an effective way to achieve multicolor.[147,148] Moon et al.[147] fabricated a flexible M-ECD by a "cut-and-stick" strategy, designing an EC chromophore gel electrolyte by uniformly mixing poly(vinylidene fluoride-co-hexafluoro-propylene) (P(VDF-co-HFP)), ionic liquids (e.g., 1-butyl-3-methylimidazolium bis(trifluoromethylsulfonyl) imide ([BMI][TFSI]), 1-butyl-3-methylimidazolium tetrafluoroborate ([BMI][BF_4])) and viologen together. The colors of the ECD can be easily tuned by the ionic liquid species due to the monomer–dimer equilibrium effects. Oh et al.[148] demonstrated a flexible M-ECD by introducing monoheptyl viologen (MHV^+) and diheptyl viologen (DHV^{2+}) into the ionic gel electrolyte. Though the chemical structures of the two EC chromophores are similar, the EC behavior is significantly different when mixed due to the different color change potential. As a result, the fabricated flexible ECDs can show three colors of yellowish, blue, and magenta. In addition, the M-ECDs also have an excellent CE of 87.5 cm^2 C^{-1} (magenta) and 91.3 cm^2 C^{-2} (blue) with a low power consumption of 248 μW cm^{-2} (magenta) and ~72 μW cm^{-2} (blue), showing that the voltage-tunable M-ECDs are very promising in low-power displays. To
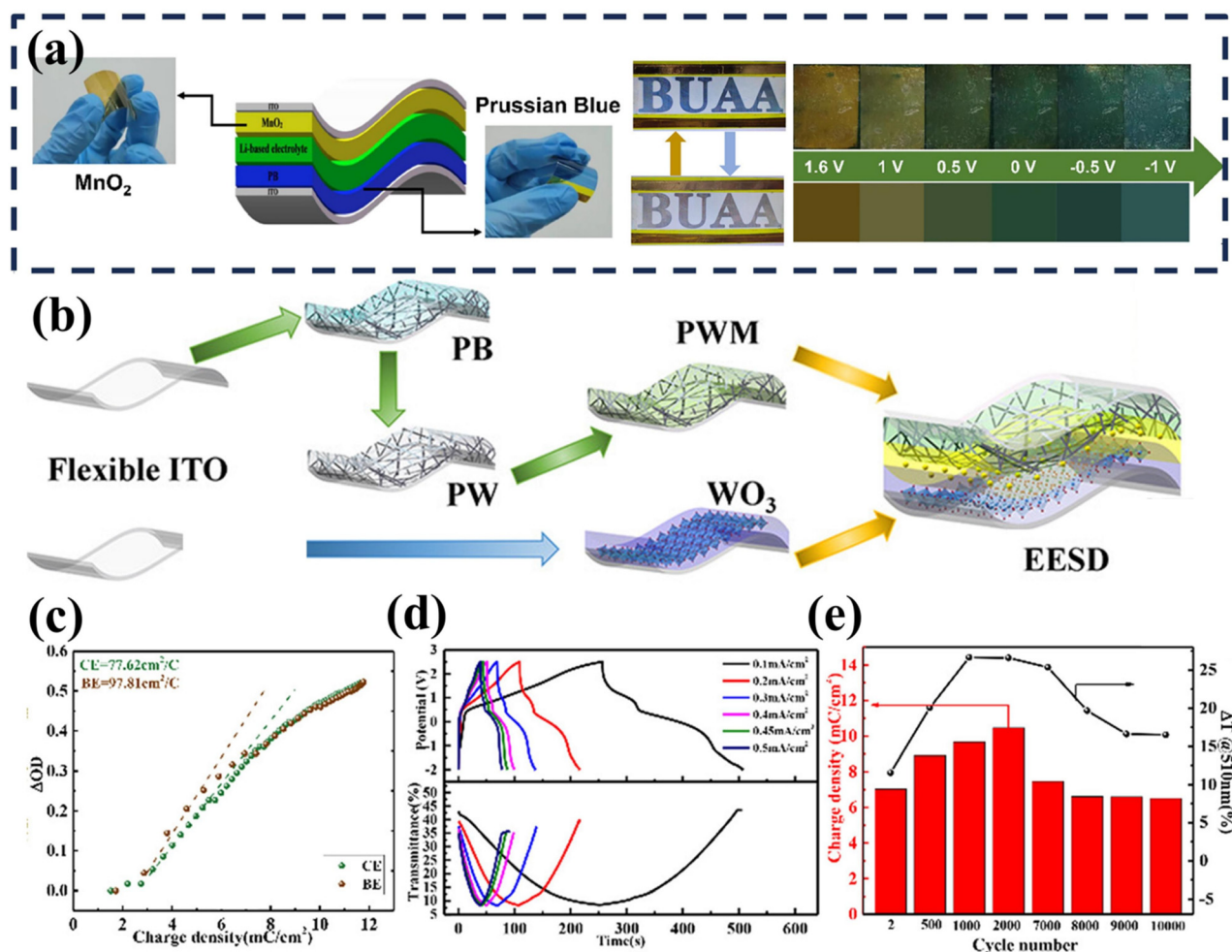
Fig. 6 (a) Schematic diagram of the flexible M-ECD and real photos (up) and emulation images (down) at different voltages. Reproduced with permission.[133] Copyright 2023 American Chemical Society. Schematic illustration (b) and relevant characterizations (c–e) of the present EESD. Reproduced with permission. Copyright 2022 American Chemical Society.

further improve the coloration and charge dissipation of M-ECDs, Liu et al.[149] fabricated a flexible M-ECD by using a multicolor PANI electrode and 1-methyl-4,4′-bipyridyl iodide (MBI). The MBI can act as both electrolyte and cathodic EC layer, which can simplify the structure and enrich the color of the ECD. As a result, the device can display a wide color range (red, yellow, green, blue, and purple) with a wide band optical modulation (58.1% at 550 nm and 35% at 800 nm), fast switching time of 1 s/1.9 s (modulating 77%-colored/bleached), and high CE of 140.6 cm^2 C^{-1}.

3.3.3 Integration with structural color.

Structural colors are generated by the interaction of the micro- and nanostructures of a material with incident light. The main structures of artificial structural colors include photonic crystals, Fabry–Pérot (F–P) microcavities and metasurfaces, etc.[150] A photonic crystal is a periodic dielectric structure in which light of a given wavelength within the bandgap of the photonic crystal is completely reflected, thereby displaying the corresponding color.[151] Metasurfaces can achieve optical confinement by modulating the phase, amplitude and polarization of the incident electro-

magnetic wave.[152] Among them, F–P cavities have gained more attention because the preparation process is simple and they are easy to compact, showing promising applications in designing certain optical devices, including modulators, tunable optical filters, and pressure sensors.[70,153,154] Generally, F–P cavities consist of reflective–dielectric–reflective symmetric structures, which can selectively absorb/reflect a certain wavelength of visible light through resonance, thus displaying a specific structural color.[155] Recently, some pioneer works have been proposed to combine the F–P cavity with EC materials to enrich the color tunability of ECDs.[70,156] For example, Chen et al.[156] reported the first Fabry–Pérot (F–P) cavity-type M-ECDs based only on tungsten oxide material. The electrode consists of an ITO/PET substrate, a W layer, and a WO$_3$ layer (Fig. 7a). The assembled device can display a wide variety of colors according to the different charge/discharge states (Fig. 7b) and excellent EC behaviors, including high CE (140 cm^2 C^{-1}) and fast switching responses. Rao et al.[155] constructed a flexible bilayered F–P cavity multicolor tunable ECD by using WO$_3$ as an EC layer, metal W as a partially reflective
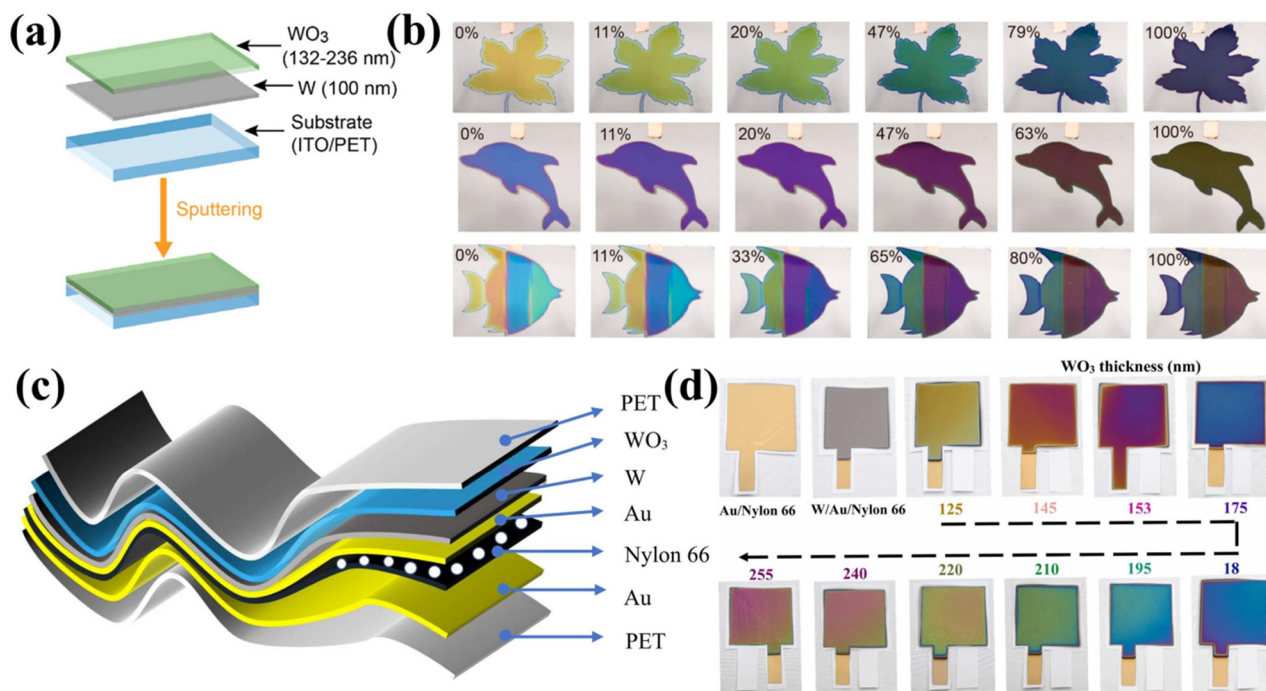
Fig. 7 (a) Preparation and mechanism of the F−P cavity-type electrochromic supercapacitor electrodes; (b) full-device fabrication with fantastic patterns. Reproduced with permission.[143] Copyright 2020 American Chemical Society. (c) Schematic structure of M-ECD; (d) corresponding optical images of devices with WO₃ layers of different thicknesses. Reproduced with permission.[142] Copyright 2023 Elsevier B.V.

layer, and metal Au as a fully reflective conductive layer. By adjusting the thickness of the WO₃ layer, multiple colors such as yellow, fuchsia, purple, blue, green, olive, and peach can be obtained (Fig. 7c and d). The device also demonstrated an excellent EC behavior, and a more precise color can be tuned by applying a different voltage with a fast color switching time of 2.1 s/2.7 s (coloring/bleaching). Similarly, by combining the EC material WO₃ with other reflective metal layers, including Ag,[157] Al,[158] and Cu,[159] F−P cavity-type multicolor ECDs can also be constructed. This strategy can overcome the shortcoming of the WO₃ in multicolor displays and greatly promote its application in flexible reflective displays and dynamic camouflage.

3.4 Flexible smart windows

The intensification of the energy crisis is a consequence of the increase in global energy demand. In response, there has been a continued exploration of renewable energy sources and energy-saving technology. As a manually operated device designed to control the level of light entering a building, EC-based smart windows have received much attention in academic and industry due to their potential to reduce the buildings' energy consumption and improve the energy efficiency.[160] Though several products have been successfully commercialized in the market, the conventional EC smart windows still suffer from issues of high cost, complexity, rigidity, long response time and inferior cycling stability. Compared with rigid smart windows, flexible EC-based smart windows are lightweight and can be glued to curved architectural structures due to their excellent mechanical stability, which is more

convenient for practical applications.[161] For instance, Koo *et al.*[162] demonstrated a flexible EC-based smart window by using an amorphous-quantized WO₃·H₂O modified ITO/PEN as EC electrode, LiClO₄/PMMA as gel electrolyte, and a H₂PtCl₆·6H₂O modified ITO/PEN as counter-electrode. The amorphous-quantized WO₃·H₂O can provide abundant active sites and oxygen deficiencies, which can boost the charge transfer and buffer the stress during the coloration/bleaching process. As a result, the prepared flexible ECDs manifest an excellent flexibility with a bending radius of 1.3 cm and superior bendability maintaining 76.1% of the initial optical modulation after 300 bending cycles. To overcome the poor conductivity and high charge transport barrier, Nguyen *et al.*[163] prepared a WO₃/Ti₃C₂Tₓ MXene hybrid film by a spraying method and further fabricated a large-size flexible smart window. Owing to the introduction of highly conductive 2D MXene, the charge transport barrier of WO₃-based ECD is greatly reduced, thus displaying a significantly improved EC behavior with an optical modulation of 57.6%, a CE of 126 cm² C⁻¹ and fast switching times of 1.5 s/2.7 s (bleaching/coloration). In addition, this strategy is very suitable for scale-up; as shown in Fig. 8a, a device with an area of 15 × 15 cm can be successfully constructed and demonstrated.

Recently, ITO/PET-free flexible ECDs have attracted tremendous interest due to the limitations of intrinsic brittleness and high cost of ITO, as well as poor adhesion of ITO on PET. For example, Wang *et al.*[164] reported a flexible EC electrode by electrochemically depositing a homogeneous WO₃ film on a flexible Ag nanofiber network-based transparent conductor. The
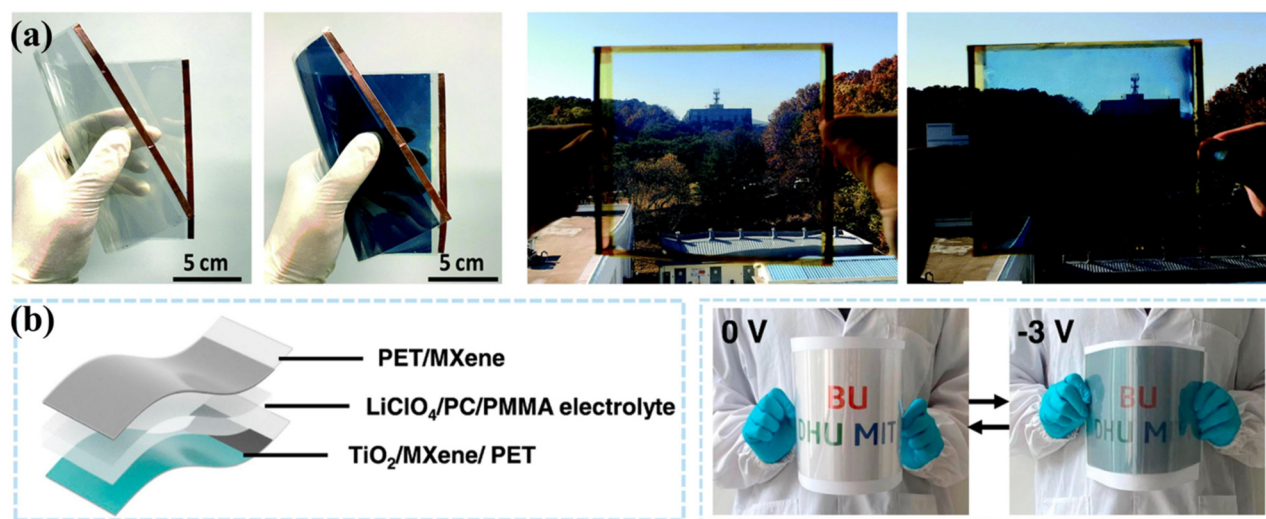
Fig. 8 (a) Photograph images of a flexible EC smart window. Reproduced with permission.[150] Copyright 2021 Royal Society of Chemistry. (b) Schematic diagram and large-area applications (about 20 × 30 cm) of the flexible solid ECD. Reproduced with permission.[151] Copyright 2021 Springer Nature.

sandwich structure of $WO_3/Ag/WO_3$ not only can improve the electrochemical stability in the oxidizing electrolyte, but also can homogenize the electrodeposition of WO_3 in the gaps among the Ag networks. The obtained hybrid EC film exhibits a high optical modulation of 89.7% and excellent cycling stability without damage after 200 bending cycles. The fabricated flexible all-solid-state ECD can color uniformly under −1 V and be pasted on any curved surface, showing practical applicability in sunglasses and smart windows. To improve the electrochemical stability of Ag, Cai et al.[165] coated the Ag grid with a PEDOT:PSS protection layer. The prepared transparent conductor displays excellent stability without obvious conductivity degradation after 2 months and superior bendability with only 7.5% optical modulation degradation after 1200 bending cycles. The fabricated flexible ECD exhibits a large optical modulation of 81.9% and high CE of 124.5 $cm^2\ C^{-1}$, manifesting promising application in flexible electronics and optoelectronic devices.

Apart from the metal nanowires/grids-based flexible EC smart windows, MXene-based transparent conductors and flexible smart windows have also attracted tremendous attention recently. For example, Li et al.[166] reported an all-MXene-based flexible EC smart window, where MXene ($Ti_3C_2T_x$)-derived 2D TiO_2 and transparent MXene film were used as a flexible EC layer and flexible conductor, respectively. The assembled 2D $TiO_2/Ti_3C_2T_x$ heterostructures possess well-balanced porosity and good interconnection, which endowed the EC electrode with fast ion/electron transport, and excellent mechanical and electrochemical stability. As a result, the fabricated flexible solid ECD can deliver excellent cycling stability showing 92% transmittance modulation retention after 1000 EC cycles. In addition, the flexible solid device can be easily scaled up, and a large-area size device of 30 × 20 cm^2 can be readily constructed, demonstrating practical large-area applications in next-generation flexible smart windows and wearable opto-electronics (Fig. 8b).

3.5 Other types of flexible multifunctional ECD

Apart from the above illustrated examples, other types of flexible multifunctional ECD have also been constructed to meet the different demands in recent years, which greatly broadens the practical applications of flexible multifunctional ECDs in electronics and optoelectronics. For example, conventional ECDs can only work in a limited temperature range due to the poor ionic conductivity of the electrolyte and macroscopic phase separation issues between electrodes/electrolytes at extreme temperatures (below 0 °C and above 60 °C). To overcome these issues, Poh et al.[167] formulated polymerized iono-gels by the one-step photopolymerization of vinyl-functiona-lized ionic liquids (BVIMTFSI), acrylate-terminated cross-linking agents (PEGDA700), and 1,3-ethylmethylimidazolium bis(trifluoromethylsulfonyl)imide (EMIMTFSI) ionic liquid. The designed ionogel electrolyte exhibits excellent transparency and stretchability, and possessed superior physico-chemical stability (air, thermal and electrochemical stability), manifesting excellent thermally robust behavior in various conditions. The as-fabricated flexible ECD achieved a fast switching time (1.5/1.9 s at 572 nm), high color contrast (45.2% and 56.4%), excellent cycling stability (90% contrast retention after 3000 switching cycles), and wide temperature operation (−20 to 100 °C). Qiu et al.[77] reported a transparent flexible ethylene glycol-assisted polyvinyl alcohol (PVA) based hydrogel electrolyte with Zn^{2+} and Al^{3+} as co-charge carrier. As shown in Fig. 9a–c, the obtained hydrogel electrolyte can deliver a high ionic conductivity of 2.9 mS cm^{-1} and 4.5 × 10^{-2} mS cm^{-1} with a transmittance of 94% and 94.3% at 60 °C and −40 °C, respectively. In addition, the hydrogel electrolyte has the merits of low cost, facile preparation, and good physico-
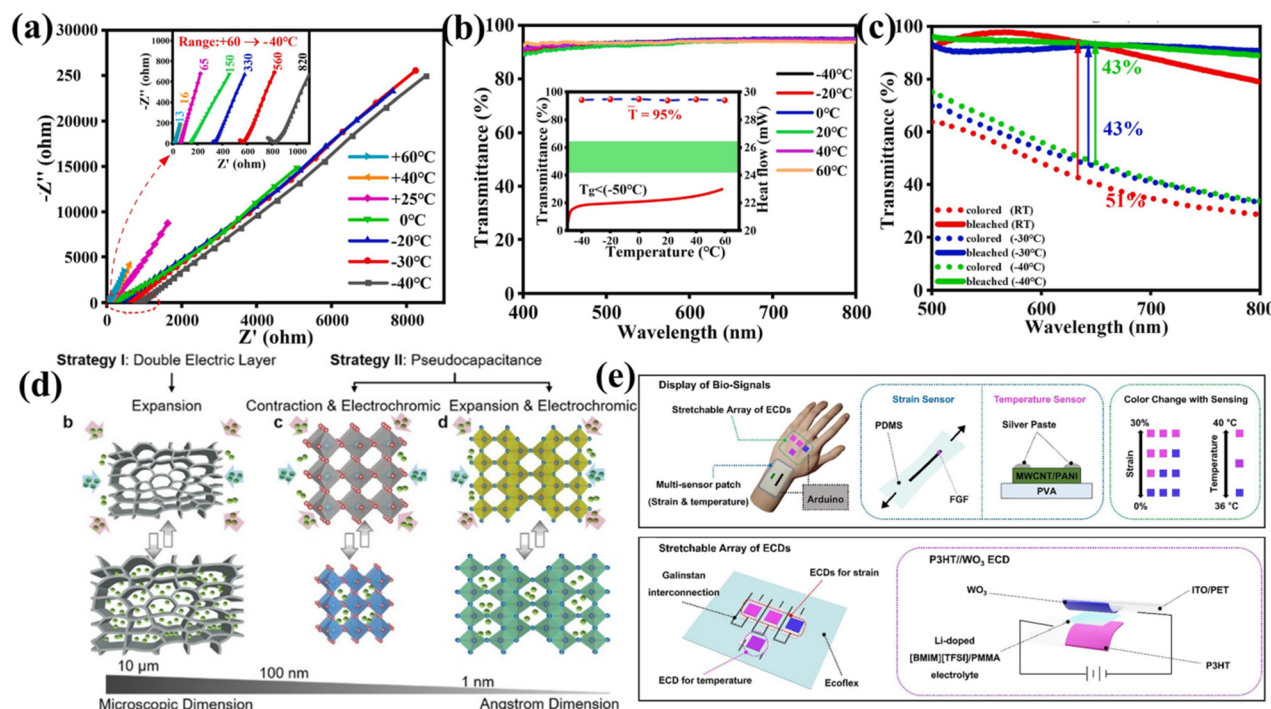
Fig. 9 (a–c) Various tests of the PVA-based hydrogel at various temperatures. Reproduced with permission.[74] Copyright 2023 Elsevier Ltd. (d) Diagram of the actuation in microporous structure induced by the ionic adsorption/desorption and synchronous color change and actuation induced by the lattice contraction and expansion. Reproduced with permission.[156] Copyright 2022 Wiley-VCH GmbH. (e) Schematic illustration of a skin-attached multi-sensor. Reproduced with permission.[43] Copyright 2023 Elsevier B.V.

chemical stability. The assembled flexible $Al/W_{10}O_{49}$ ECD can work well at a low temperature of −40 °C with high optical modulation of 43% at 633 nm.

Due to the potential application in biomimetic dual-stealth camouflage, robotics, and biomedicine, EC-actuators also have garnered significant attention and have been developed rapidly over the past few years. However, traditional ITO/glass transparent conductors are rigid, and can hardly demonstrate actuation. To address this issue, Li et al.[168] designed an EC-actuator by employing PEDOT:PSS-protected Ag nanowires as a transparent conductor and $W_{10}O_{49}$ nanowires as an EC layer. Benefiting from the lattice contraction/recovery induced by the reversible Li^+ intercalation/deintercalation into the $W_{10}O_{49}$ nanowires, the formed bifunctional film displays impressive EC and actuator behaviors with a fast-switching time of 4.1/2.9 s (coloration/bleaching), high CE of 119.2 cm^2 C^{-1}, and excellent actuation performance with a largest bending angle of 238° at 5 s. To further extend the dual-responsive color/shape change mode, Ling et al.[169] reported a back-to-back structure multicolor EC-actuator by depositing V_2O_5 nanowires and single-walled CNTs on a porous polymer membrane, where the V_2O_5 and CNTs were used as multicolor EC materials and conductive current collectors. Owing to the lattice expansion/recovery of V_2O_5 nanowires induced by the reversible de-/intercalation of Li^+, the composite film exhibits a synchronous color change (yellow, green and dark turquoise-blue) and actuation (Fig. 9d). The air-working EC-actuator can be easily

fabricated by using two composite films stacked together. The produced device can also show a high actuation distance about ±9.7 mm with a reversible color change between yellow and green.

The traditional sensors are connected by signal processors and display devices together with an external electric circuit, which makes it difficult to realize portable wearable applications. In contrast, ECDs can visually display the strength of sensor signals through color changes, so the combination of EC technology and sensor technology can directly identify the sensor information by the naked eye.[170,171] For example, Kim et al.[45] reported an interactive display system by integrating EC devices and temperature and strain sensors together, which can visually display the skin temperature and wrist movement. The EC materials can change color between magenta, violet, and blue at −1.5 V, 0.5 V, and 1.5 V, respectively. With this EC sensor system, the wrist bending and temperature change of the skin can induce the color change in the ECD patterns. This work suggests the potential application of stretchable arrays of ECDs to effective interactive skin-attachable display devices for multi-sensor signals (Fig. 9e).

4 Conclusion and perspectives

In recent years, with the significant development of wearable and portable electronics, the interest in flexible multifunc-

tional ECDs is growing rapidly. Compared with the traditional rigid glass-based ECDs, flexible multifunctional ECDs provide better functionality and can be easily integrated with curved surfaces. This review systematically discusses the recent advances in flexible multifunctional ECDs, including flexible self-powered ECDs, flexible ECESDs, flexible M-ECDs, and flexible smart windows. The configuration of flexible ECDs, design principles, integration mechanisms, and material optimization are also discussed. However, the flexible multifunctional ECDs are still in their infancy, and more effort should be devoted to address the issues of scalability, cost, device delamination, dissociation and degradation before the practical application. The first challenge is to reduce the cost of flexible multifunctional ECDs. Currently, the most popular flexible transparent conductor is ITO/PET due to its high optical transparency and electronic conductivity. However, the costly preparation process and rare indium as well as poor adhesion between ITO and PET limit its further use in flexible ECDs. As an alternative, ITO-free transparent conductors, including metal nanowires, conducting polymers, carbon materials, and MXene, have made significant progress in recent years. Unfortunately, the comprehensive performance, including transparency, electronic conductivity, and electrochemical stability, still cannot compete with ITO. The second challenge is to improve the cycling stability and deformability of flexible multifunctional ECDs. Unlike the conventional rigid ECDs, the flexible multifunctional ECDs need to work repeatedly under static, bending, twisting and stretching conditions, which easily induce electrochemical performance deterioration due to the delamination and electrolyte leakage. Therefore, more attention needs to be paid to improving the adhesion stability by introducing chemical bonds or electrostatic interactions between different layers, to satisfy the various working conditions. The third challenge is the mass production of EC materials with low cost, good EC performance, and a facile preparation process. Currently, the most popular synthesis methods are hydrothermal, electrodeposition, sol–gel, electrospinning, *etc*., which are costly and still limited to the laboratory scale. There is an urgent need for a breakthrough in large-scale preparation methods with acceptable cost, easy morphology control, and quantity regulation. In addition, current EC materials are at the nanoscale, and unpredictable and irreversible side reactions often occur during the coloration/bleaching process due to the large active surface area. Therefore, the in-depth understanding of the side reactions by using advanced *in situ* characterization methods, including *in situ* X-ray diffraction, and *in situ* Raman/infrared spectroscopy, needs to be further investigated. The fourth challenge is to design solid-state electrolytes with high ionic conductivity and thermal stability, excellent electrochemical inertness, and outstanding deformability. To avoid the leakage of liquid electrolyte, solid-state electrolytes are more practical for flexible multifunctional ECDs. However, currently reported solid-state electrolytes have poor ionic conductivity and are easily cracked under mechanical strain/stress. Therefore, more effort needs to be paid to the design of high ionic conductivity,

stretchable, and self-healing solid-state electrolytes to meet the demands of various types of deformable ECD. Last but not least is that the scale-up method must be reliable according to industrial manufacturing standards. To date, the most widely reported methods, including electrodeposition, spray coating, spin coating, and rod coating, are still limited to the laboratory scale, and large-scale methods with controllable thickness and uniformity need to be further developed. Therefore, practical adaptations to industrial manufacturing standards need to be developed, which requires the collaboration between industry and academia. Overall, the further development of flexible multifunctional ECDs requires a systematic optimization of transparent conductors, EC materials, electrolytes, sealing and packaging materials, and device structure design. We believe that with the continuous performance improvement in flexible multifunctional ECDs by the optimization and integration of different EC materials, design of hybrid approaches, in-depth understanding of the mechanism, and development of fabrication technologies, the practical applications will proliferate in the near future.

Author contributions

All authors conceptualized, curated data, wrote, reviewed and edited the manuscript before submission.

Data availability

No new data were created or analyzed in this study.

Conflicts of interest

There are no conflicts to declare.

Acknowledgements

References

1 R. Zheng, Y. Wang, C. Jia, Z. Wan, J. Luo, H. A. Malik, X. Weng, J. Xie and L. Deng, *ACS Appl. Mater. Interfaces*, 2018, **10**, 35533–35538.
2 A. K. Sasmal and T. Pal, *J. Indian Chem. Soc.*, 2021, **98**, 100073.
3 J. H. Day, *Chem. Rev.*, 1963, 65–80.
4 T. Yamase, *Chem. Rev.*, 1998, **98**, 307–326.
5 M. Irie, T. Fukaminato, K. Matsuda and S. Kobatake, *Chem. Rev.*, 2014, **114**, 12174–12277.
6 R. J. Mortimer, *Chem. Soc. Rev.*, 1997, **26**, 147.

7 S. J. Lee, T.-G. Lee, S. Nahm, D. H. Kim, D. J. Yang and S. H. Han, *J. Alloys Compd.*, 2020, **815**, 152399.

8 Y. Zhang, B. Xu, F. Zhao, H. Li, J. Chen, H. Wang and W. W. Yu, *FlexMat*, 2024, **1**, 23–45.

9 J. R. Platt, *J. Chem. Phys.*, 1961, **34**, 862–863.

10 S. K. Deb, *Appl. Opt.*, 1969, **8**(Suppl 1), 192–195.

11 J. Svensson and C. G. Granqvist, *Thin Solid Films*, 1985, **126**, 31–36.

12 C.-J. Tang, J.-M. Ye, Y.-T. Yang and J.-L. He, *Opt. Mater.*, 2016, **55**, 83–89.

13 S. Huang, Y. Liu, M. Jafari, M. Siaj, H. Wang, S. Xiao and D. Ma, *Adv. Funct. Mater.*, 2021, **31**, 2010022.

14 H. Gong, A. Li, G. Fu, M. Zhang, Z. Zheng, Q. Zhang, K. Zhou, J. Liu and H. Wang, *J. Mater. Chem. A*, 2023, **11**, 8939–8949.

15 J. Li, A. Levitt, N. Kurra, K. Juan, N. Noriega, X. Xiao, X. Wang, H. Wang, H. N. Alshareef and Y. Gogotsi, *Energy Storage Mater.*, 2019, **20**, 455–461.

16 J. Kim, M. Rémond, D. Kim, H. Jang and E. Kim, *Adv. Mater. Technol.*, 2020, **5**, 1900890.

17 L. Wang, M. Guo, J. Zhan, X. Jiao, D. Chen and T. Wang, *J. Mater. Chem. A*, 2020, **8**, 17098–17105.

18 X. Yu, P. Guo, J. Chen, S. Li and H. Li, *Responsive Mater.*, 2024, **2**, e20240013.

19 J. Yan, S. Li, B. Lan, Y. Wu and P. S. Lee, *Adv. Funct. Mater.*, 2019, **30**, 1902564.

20 Z. Wang, X. Wang, S. Cong, F. Geng and Z. Zhao, *Mater. Sci. Eng., R*, 2020, **140**, 100524.

21 L. Manjakkal, L. Pereira, E. Kumi Barimah, P. Grey, F. F. Franco, Z. Lin, G. Jose and R. A. Hogg, *Prog. Mater. Sci.*, 2024, **142**, 101244.

22 H. Wang, C.-J. Yao, H.-J. Nie, L. Yang, S. Mei and Q. Zhang, *J. Mater. Chem. C*, 2020, **8**, 15507–15525.

23 W. Wu, S. Guo, J. Bian, X. He, H. Li and J. Li, *J. Energy Chem.*, 2024, **93**, 453–470.

24 A. L. S. Eh, A. W. M. Tan, X. Cheng, S. Magdassi and P. S. Lee, *Energy Technol.*, 2017, **6**, 33–45.

25 B. Wang, W. Zhang, F. Zhao, W. W. Yu, A. Y. Elezzabi, L. Liu and H. Li, *Nano Mater. Sci.*, 2023, **5**, 369–391.

26 A. L.-S. Eh, J. Chen, X. Zhou, J.-H. Ciou and P. S. Lee, *ACS Energy Lett.*, 2021, **6**, 4328–4335.

27 D. He, C. Su, C. Zhao, G. Yan, Z. Zhao and W. Mai, *Chem. Eng. J.*, 2022, **438**, 135469.

28 W. Li, T. Bai, G. Fu, Q. Zhang, J. Liu, H. Wang, Y. Sun and H. Yan, *Sol. Energy Mater. Sol. Cells*, 2022, **240**, 111709.

29 A. Viñuales, Y. Alesanco, G. Cabañero, J. Sobrado and R. Tena-Zaera, *Sol. Energy Mater. Sol. Cells*, 2017, **167**, 22–27.

30 R. Brooke, E. Mitraka, S. Sardar, M. Sandberg, A. Sawatdee, M. Berggren, X. Crispin and M. P. Jonsson, *J. Mater. Chem. C*, 2017, **5**, 5824–5830.

31 P. Cossari, A. Cannavale, S. Gambino and G. Gigli, *Sol. Energy Mater. Sol. Cells*, 2016, **155**, 411–420.

32 H. Lee, M. Kim, I. Kim and H. Lee, *Adv. Mater.*, 2016, **28**, 4541–4548.

33 W. Kang, C. Yan, C. Y. Foo and P. S. Lee, *Adv. Funct. Mater.*, 2015, **25**, 4203–4210.

34 W. Kang, M. F. Lin, J. Chen and P. S. Lee, *Small*, 2016, **12**, 6370–6377.

35 G. Fu, H. Gong, T. Bai, Q. Zhang and H. Wang, *J. Mater. Sci.: Mater. Electron.*, 2023, **34**, 1316.

36 C. Miao, H. Du, X. Zhang and H. V. Tippur, *Cellulose*, 2021, **29**, 557–569.

37 A. W. Lang, A. M. Österholm and J. R. Reynolds, *Adv. Funct. Mater.*, 2019, **29**, 1903487.

38 Y. Djaoued, V. H. Phong, S. Badilescu, P. V. Ashrit, F. E. Girouard and V.-V. Truong, *Thin Solid Films*, 1997, **293**, 108–112.

39 S. Macher, M. Rumpel, M. Schott, U. Posset, G. A. Giffin and P. Löbmann, *ACS Appl. Mater. Interfaces*, 2020, **12**, 36695–36705.

40 W. Li, J. Sun, J. Zhang, O. A. Ganiyat and Y. Cui, *Results Surf. Interfaces*, 2021, **2**, 100002.

41 G. Cai, J. Wang and P. S. Lee, *Acc. Chem. Res.*, 2016, **49**, 1469–1476.

42 S. Huang, Y. Liu, F. Yang, Y. Wang, T. Yu and D. Ma, *Environ. Chem. Lett.*, 2022, **20**, 3005–3037.

43 Z. Ke, A. Abtahi, J. Hwang, K. Chen, J. Chaudhary, I. Song, K. Perera, L. You, K. N. Baustert, K. R. Graham and J. Mei, *J. Am. Chem. Soc.*, 2023, **145**, 3706–3715.

44 B. Wu, Y. Guo, C. Hou, Q. Zhang, Y. Li and H. Wang, *Nano Energy*, 2021, **89**, 106487.

45 D. S. Kim, Y. H. Lee, J. W. Kim, H. Lee, G. Jung and J. S. Ha, *Chem. Eng. J.*, 2022, **429**, 132289.

46 C. Ma, H. Liu, C. Teng, L. Li, Y. Zhu, H. Yang and L. Jiang, *ACS Appl. Mater. Interfaces*, 2020, **12**, 55372–55381.

47 H. Peng, M. Pan, H. Jiang, W. Huang, X. Wang, Q. Yang, S. Chen and B. Yan, *ACS Appl. Mater. Interfaces*, 2022, **14**, 42402–42411.

48 S. Guo, R. Zhu, J. Chen, W. Liu, Y. Zhang, J. Li and H. Li, *Microsyst. Nanoeng.*, 2024, **10**, 89.

49 J. Zhao, S. Zhang, S. Chang, C. Li, C. Fang, X. Xia, L. Shen, J. Yang Lee, C. Cao, X. Zhang and Y. Xuan, *Chem. Eng. J.*, 2024, **480**, 148010.

50 D. A. Barus, K. Sebayang, J. Ginting and R. T. Ginting, *J. Phys.: Conf. Ser.*, 2018, **1116**, 032006.

51 H. Zhang, J. Feng, F. Sun, D. Zhou, G. Cao, Z. Wu, S. Wang, F. Su, Y. Tian and Y. Tian, *Adv. Mater.*, 2023, **4**, 995–1004.

52 G. Cai, S. Park, X. Cheng, A. L.-S. Eh and P. S. Lee, *Sci. Technol. Adv. Mater.*, 2018, **19**, 759–770.

53 W. Zhao, J. Wang, B. Tam, H. Zhang, F. Li, A. Du and W. Cheng, *Adv. Opt. Mater.*, 2023, **11**, 2202774.

54 S. Weng, Z. Cao, K. Song, W. Chen, R. Jiang, A. A. Rogachev, M. A. Yarmolenko, J. Zhou and H. Zhang, *ACS Appl. Mater. Interfaces*, 2024, **16**, 18164–18172.

55 C.-T. Lee, S. Han, Y.-X. Zhao, Y.-C. Hung, T.-H. Hsu, H.-Y. Hsieh and K.-W. Weng, *Surf. Coat. Technol.*, 2019, **363**, 426–429.

56 Y. Liang, S. Cao, Q. Wei, R. Zeng, J. Zhao, H. Li, W. W. Yu and B. Zou, *Nano-Micro Lett.*, 2021, **13**, 196.

57 S. Huang, R. Zhang, P. Shao, Y. Zhang and R.-T. Wen, *Adv. Opt. Mater.*, 2022, **10**, 2200903.

58 R. Goel, R. Jha and C. Ravikant, *Chem. Pap.*, 2023, **77**, 2885–2903.

59 S. H. Sutar, B. M. Babar, K. B. Pisal, A. I. Inamdar and S. H. Mujawar, *J. Energy Storage*, 2023, **73**, 109035.

60 D. Ma, A. Lee-Sie Eh, S. Cao, P. S. Lee and J. Wang, *ACS Appl. Mater. Interfaces*, 2022, **14**, 1443–1451.

61 J. Wang, W. Zhao, B. Tam, H. Zhang, Y. Zhou, L. Yong and W. Cheng, *Chem. Eng. J.*, 2023, **452**, 139655.

62 H. Sun, W. Wang, Y. Xiong, Z. Jian and W. Chen, *Chin. Chem. Lett.*, 2024, **35**, 109213.

63 D. Zhang, J. Wang, Z. Tong, H. Ji and H. Y. Qu, *Adv. Funct. Mater.*, 2021, **31**, 2106577.

64 J. Wang, J. Liu, M. Hu, J. Zeng, Y. Mu, Y. Guo, J. Yu, X. Ma, Y. Qiu and Y. Huang, *J. Mater. Chem. A*, 2018, **6**, 11113–11118.

65 C. S. Pinto, V. H. R. Souza, A. Schmidt and A. J. G. Zarbin, *Synth. Met.*, 2023, **293**, 117259.

66 Y. Luo, J.-P. Liu, L.-K. Li and S.-Q. Zang, *Inorg. Chem.*, 2023, **62**, 14385–14392.

67 Y. Sui, Y. Ma, Y. Gao, J. Song, Y. Ye, H. Niu, W. Ma, P. Zhang and C. Qin, *New J. Chem.*, 2021, **45**, 10654–10663.

68 K.-C. Lee, C.-W. Chang-Jian, E.-C. Cho, J.-H. Huang, W.-T. Lin, B.-C. Ho, J.-A. Chou and Y.-S. Hsiao, *Sol. Energy Mater. Sol. Cells*, 2019, **195**, 1–11.

69 E. Eren, M. F. Aydın and A. U. Oksuz, *J. Solid State Electrochem.*, 2020, **24**, 1057–1065.

70 Z. Wang, X. Wang, S. Cong, J. Chen, H. Sun, Z. Chen, G. Song, F. Geng, Q. Chen and Z. Zhao, *Nat. Commun.*, 2020, **11**, 302.

71 W. Zhang, H. Li, E. Hopmann and A. Y. Elezzabi, *Nanophotonics*, 2020, **10**, 825–850.

72 Q. Wang, S. Cao, Q. Meng, K. Wang, T. Yang, J. Zhao and B. Zou, *Mater. Horiz.*, 2023, **10**, 960–966.

73 X. Liu, T. Cao, W. Yao, L. Shen, J. Xu, F. Jiang and Y. Du, *J. Colloid Interface Sci.*, 2020, **570**, 382–389.

74 W. Zhang, H. Li, W. W. Yu and A. Y. Elezzabi, *Light: Sci. Appl.*, 2020, **9**, 121.

75 V. Primiceri, M. Pugliese, C. T. Prontera, A. G. Monteduro, M. Esposito, A. Maggiore, A. Cannavale, R. Giannuzzi, G. Gigli and V. Maiorano, *Sol. Energy Mater. Sol. Cells*, 2022, **240**, 111657.

76 P. Barbosa, L. Rodrigues, M. Silva, M. Smith, A. Gonçalves and E. Fortunato, *J. Mater. Chem.*, 2010, **20**, 723–730.

77 B. Qiu, X. Xiao, G. Xu and G. Dong, *Mater. Today Chem.*, 2023, **33**, 101703.

78 B. Xu, J. Chen, Z. Ding, J. Hu, Y. Zhang, H. Li and H. Wang, *Small Sci.*, 2023, **3**, 2300025.

79 M. Han, C. H. Cho, H. Jang and E. Kim, *J. Mater. Chem. A*, 2021, **9**, 16016–16027.

80 C. Gu, A.-B. Jia, Y.-M. Zhang and S. X.-A. Zhang, *Chem. Rev.*, 2022, **122**, 14679–14721.

81 N. C. Davy, M. Sezen-Edmonds, J. Gao, X. Lin, A. Liu, N. Yao, A. Kahn and Y.-L. Loo, *Nat. Energy*, 2017, **2**, 17104.

82 A. Cánovas-Saura, R. Ruiz, R. López-Vicente, J. Abad, A. Urbina and J. Padilla, *Electron. Mater.*, 2021, **2**, 174–185.

83 H. Zhang, F. Sun, J. Feng, H. Ling, D. Zhou, G. Cao, S. Wang, F. Su, Y. Tian and Y. Tian, *Cell Rep. Phys. Sci.*, 2022, **3**, 101193.

84 Z. He, B. Gao, T. Li, J. Liao, B. Liu, X. Liu, C. Wang, Z. Feng and Z. Gu, *ACS Sustainable Chem. Eng.*, 2018, **7**, 1745–1752.

85 S. Bi, W. Jin, X. Han, X. Cao, Z. He, K. Asare-Yeboah and C. Jiang, *Nano Energy*, 2022, **102**, 107629.

86 J. Huang, Z. Ren, Y. Zhang, P. W.-K. Fong, H. T. Chandran, Q. Liang, K. Yao, H. Tang, H. Xia, H. Zhang, X. Yu, Z. Zheng and G. Li, *Adv. Energy Mater.*, 2022, **12**, 2201042.

87 L. Zhou, D. Liu, L. Liu, L. He, X. Cao, J. Wang and Z. L. Wang, *Research*, 2021, **2021**, 4673028.

88 S. Zhao, X. Gao, L. Chen, W. Huang and Y. Liu, *Appl. Mater. Today*, 2022, **28**, 101543.

89 H. Gong, S. Wang, M. Xie and H. Wang, *Sol. Energy Mater. Sol. Cells*, 2022, **248**, 112018.

90 J.-L. Wang, S.-Z. Sheng, Z. He, R. Wang, Z. Pan, H.-Y. Zhao, J.-W. Liu and S.-H. Yu, *Nano Lett.*, 2021, **21**, 9976–9982.

91 H. Li, W. Zhang and A. Y. Elezzabi, *Adv. Mater.*, 2020, **32**, 2003574.

92 Q. Ma, J. Chen, H. Zhang, Y. Su, Y. Jiang and S. Dong, *ACS Energy Lett.*, 2023, **8**, 306–313.

93 F. Zhao, C. Li, S. Li, B. Wang, B. Huang, K. Hu, L. Liu, W. W. Yu and H. Li, *Adv. Mater.*, 2024, 2405035, DOI: **10.1002/adma.202405035**.

94 J. Hu, Y. Zhang, B. Xu, Y. Ouyang, Y. Ma, H. Wang, J. Chen and H. Li, *Chem. Commun.*, 2024, **60**, 566–569.

95 Y. An, Y. Tian, C. Liu, S. Xiong, J. Feng and Y. Qian, *ACS Nano*, 2021, **15**, 15259–15273.

96 W. Nie, H. Cheng, Q. Sun, S. Liang, X. Lu, B. Lu and J. Zhou, *Small Methods*, 2024, **8**, 2201572.

97 Y. Chen, Q. Zhao, Y. Wang, W. Liu, P. Qing and L. Chen, *Electrochim. Acta*, 2021, **399**, 139334.

98 C. Xiong, T. Wang, Z. Zhao and Y. Ni, *SmartMat*, 2022, **4**, e1158.

99 P. Yang, P. Sun and W. Mai, *Mater. Today*, 2016, **19**, 394–402.

100 D. S. Dalavi, R. S. Desai and P. S. Patil, *J. Mater. Chem. A*, 2022, **10**, 1179–1226.

101 A. Amiri, A. Bruno and A. A. Polycarpou, *Carbon Energy*, 2023, **5**, e320.

102 Y. Chen, S. Li, J. Chen, L. Gao, P. Guo, C. Wei, J. Fu and Q. Xu, *J. Colloid Interface Sci.*, 2024, **664**, 360–370.

103 S. Li, Q. Tian, J. Chen, Y. Chen, P. Guo, C. Wei, P. Cui, J. Jiang, X. Li and Q. Xu, *Chem. Eng. J.*, 2023, **457**, 141265.

104 X. Jiao, G. Li, Z. Yuan and C. Zhang, *ACS Appl. Energy Mater.*, 2021, **4**, 14155–14168.

105 Y. Shi, M. Sun, Y. Zhang, J. Cui, Y. Wang, X. Shu, Y. Qin, H. H. Tan, J. Liu and Y. Wu, *Sol. Energy Mater. Sol. Cells*, 2020, **212**, 110579.

106 L. Shen, L. Du, S. Tan, Z. Zang, C. Zhao and W. Mai, *Chem. Commun.*, 2016, **52**, 6296–6299.

107 T. Hao, S. Wang, H. Xu, X. Zhang, J. Xue, S. Liu, Y. Song, Y. Li and J. Zhao, *Chem. Eng. J.*, 2021, **426**, 130840.

108 P. Zhang, Q. Sui, Z. Liu, C. Hu, C. Li, X. Guo, J. Wang and G. Cai, *Chem. Eng. J.*, 2024, **498**, 155277.

109 G. Cai, X. Cheng, M. Layani, A. W. M. Tan, S. Li, A. L.-S. Eh, D. Gao, S. Magdassi and P. S. Lee, *Nano Energy*, 2018, **49**, 147–154.

110 M. Hassan, P. Li, J. Lin, Z. Li, M. S. Javed, Z. Peng and K. Celebi, *Small*, 2024, **20**, 2400278.

111 H. Li, L. McRae, C. J. Firby, M. Al-Hussein and A. Y. Elezzabi, *Nano Energy*, 2018, **47**, 130–139.

112 P. Zhang, F. Zhu, F. Wang, J. Wang, R. Dong, X. Zhuang, O. Schmidt and X. Feng, *Adv. Mater.*, 2016, **29**, 1604491.

113 R. U. Amate, P. J. Morankar, G. T. Chavan, A. M. Teli, R. S. Desai, D. S. Dalavi and C.-W. Jeon, *Electrochim. Acta*, 2023, **459**, 142522.

114 G. Cai, R. Zhu, S. Liu, J. Wang, C. Wei, K. J. Griffith, Y. Jia and P. S. Lee, *Adv. Energy Mater.*, 2022, **12**, 2103106.

115 K. Xu, L. Wang, G. Liu, C. Ge, L. Wang, W. Wang and M. Chen, *Energy Environ. Mater.*, 2023, **6**, e12362.

116 K. Zhou, H. Wang, J. Jiu, J. Liu, H. Yan and K. Suganuma, *Chem. Eng. J.*, 2018, **345**, 290–299.

117 W. Zhang, J. Cao, H. Li, C. Du, S. Chen, L. Cao, J. Xu, B. Lu and G. Zhang, *J. Energy Storage*, 2024, **98**, 113154.

118 L. Zhang, Y. Chen, Z. Jiang, J. Chen, C. Wei, W. Wu, S. Li and Q. Xu, *Energy Environ. Mater.*, 2024, **7**, e12507.

119 L. Gao, Y. Ma and M. Cao, *Int. J. Hydrogen Energy*, 2024, **49**, 1–10.

120 L. Gao, H. Zhan, G. Feng, Y. Ma, C. Zhang, Y. Zhang and M. Cao, *J. Energy Storage*, 2024, **97**, 112890.

121 T. G. Yun, J. Lee, H. S. Kim, J. Y. Cheong, S. H. Kim, Y. Kim, S. Lee and I.-D. Kim, *Adv. Mater.*, 2023, **35**, 2301141.

122 H. Li, L. McRae, C. J. Firby and A. Y. Elezzabi, *Adv. Mater.*, 2019, **31**, 1807065.

123 Z. Tong, R. Lian, R. Yang, T. Kang, J. Feng, D. Shen, Y. Wu, X. Cui, H. Wang, Y. Tang and C.-S. Lee, *Energy Storage Mater.*, 2022, **44**, 497–507.

124 H. Li, C. J. Firby and A. Y. Elezzabi, *Joule*, 2019, **3**, 2268–2278.

125 Z. Tong, T. Kang, Y. Wan, R. Yang, Y. Wu, D. Shen, S. Liu, Y. Tang and C.-S. Lee, *Adv. Funct. Mater.*, 2021, **31**, 2104639.

126 Y. Ding, H. Sun, Z. Li, C. Jia, X. Ding, C. Li, J.-G. Wang and Z. Li, *J. Mater. Chem. A*, 2023, **11**, 2868–2875.

127 T. G. Yun, J. Lee, H. S. Kim, J. Y. Cheong, S. H. Kim, Y. Kim, S. Lee and I. D. Kim, *Adv. Mater.*, 2023, **35**, 2301141.

128 S. Sun, C. Tang, Y. Jiang, D. Wang, X. Chang, Y. Lei, N. Wang and Y. Zhu, *Sol. Energy Mater. Sol. Cells*, 2020, **207**, 110332.

129 S. B. Singh, D. T. Tran, K. U. Jeong, N. H. Kim and J. H. Lee, *Small*, 2021, **18**, 2104462.

130 G. Cai, J. Chen, J. Xiong, A. Lee-Sie Eh, J. Wang, M. Higuchi and P. S. Lee, *ACS Energy Lett.*, 2020, **5**, 1159–1166.

131 Q. Huang, J. Hu, M. Yin, Y. Zhu and R.-T. Wen, *Sol. Energy Mater. Sol. Cells*, 2024, **267**, 112706.

132 U. Linderhed, I. Petsagkourakis, P. A. Ersman, V. Beni and K. Tybrandt, *Flexible Printed Electron.*, 2021, **6**, 045014.

133 K. Tang, Y. Zhang, Y. Shi, J. Cui, X. Shu, Y. Wang, J. Liu, J. Wang, H. H. Tan and Y. Wu, *J. Mater. Chem. C*, 2018, **6**, 12206–12216.

134 H. Zhao, Y. Chen, L. Zhao, X. Liang and Z. Liu, *Sol. Energy Mater. Sol. Cells*, 2023, **257**, 112374.

135 D. Shin, J. Kim, S. Choi, G. Song, A. Rougier and C. S. Lee, *Sol. Energy Mater. Sol. Cells*, 2023, **257**, 112341.

136 J. Wu, D. Qiu, H. Zhang, H. Cao, W. Wang, Z. Liu, T. Tian, L. Liang, J. Gao and F. Zhuge, *J. Electrochem. Soc.*, 2018, **165**, D183–D189.

137 S. Sun, S. Cui, F. Wang, M. Gao, W. Wei, J. Dong, X. Xia, Q. Zhu and J. Zhang, *ACS Appl. Electron. Mater.*, 2022, **4**, 4724–4732.

138 Q. Liu, X. Ou, Y. Niu, L. Li, D. Xing, Y. Zhou and F. Yan, *Angew. Chem., Int. Ed.*, 2024, **63**, e202317944.

139 X. Huang, J. Chen, H. Xie, F. Zhao, S. Fan and Y. Zhang, *Sci. China Mater.*, 2022, **65**, 2217–2226.

140 H. Zhang, S. Ming, Y. Liang, L. Feng and T. Xu, *Int. J. Electrochem.*, 2020, **15**, 1044–1057.

141 H. Fan, K. Li, X. Liu, K. Xu, Y. Su, C. Hou, Q. Zhang, Y. Li and H. Wang, *ACS Appl. Mater. Interfaces*, 2020, **12**, 28451–28460.

142 X. Gao, Y. Wang, M. Wu, C. Zhi, J. Meng and L. Zhang, *Dyes Pigm.*, 2023, **219**, 111642.

143 Y. Ding, M. Wang, Z. Mei and X. Diao, *ACS Appl. Mater. Interfaces*, 2023, **15**, 15646–15656.

144 Y. Ding, M. Wang, Z. Mei and X. Diao, *ACS Appl. Mater. Interfaces*, 2022, **14**, 48833–48843.

145 W. Xue, Y. Zhang, F. Liu, Y. Dou, M. Yan and W. Wang, *Research*, 2023, **6**, 0227.

146 W. Zhang, H. Li and A. Y. Elezzabi, *Adv. Funct. Mater.*, 2021, **32**, 2108341.

147 H. C. Moon, C.-H. Kim, T. P. Lodge and C. D. Frisbie, *ACS Appl. Mater. Interfaces*, 2016, **8**, 6252–6260.

148 H. Oh, D. G. Seo, T. Y. Yun, C. Y. Kim and H. C. Moon, *ACS Appl. Mater. Interfaces*, 2017, **9**, 7658–7665.

149 G. Liu, Z. Wang, J. Wang, H. Liu and Z. Li, *J. Colloid Interface Sci.*, 2024, **655**, 493–507.

150 X. Ran, J. Ren, S. Zhang, Y. Wu and S. Wu, *ACS Appl. Mater. Interfaces*, 2023, **15**, 41763–41771.

151 Q. Zhang, X. Li, M. Qin, F. Guan, Y. Gong, R. Wang, J. Xu and G. Chen, *ACS Appl. Electron. Mater.*, 2021, **3**, 4441–4447.

152 L. Li, Z. Yu, C. Ye and Y. Song, *Adv. Funct. Mater.*, 2024, **34**, 2311845.

153 F. J. Rodriguez, D. E. Aznakayeva, O. P. Marshall, V. G. Kravets and A. N. Grigorenko, *Adv. Mater.*, 2017, **29**, 1606372.

154 J. Zhao, M. Qiu, X. Yu, X. Yang, W. Jin, D. Lei and Y. Yu, *Adv. Opt. Mater.*, 2019, **7**, 1900646.

155 A. Rao, S. Zhang, J. Hu, L. Zheng, Q. Yao, K. Lin, C. Niu, L. Wang, M. Yang, Y. Lv and Q. Chen, *J. Alloys Compd.*, 2023, **969**, 172310.

156 J. Chen, Z. Wang, Z. Chen, S. Cong and Z. Zhao, *Nano Lett.*, 2020, **20**, 1915–1922.

157 J. Chen, Y. Li, T. Zhang, X. Zha, X. Tang, X. Mu, P. Sun, G. Song, S. Cong, Q. Chen and Z. Zhao, *Laser Photonics Rev.*, 2022, **16**, 2200303.

158 L. Zheng, S. Zhang, Q. Yao, K. Lin, A. Rao, C. Niu, M. Yang, L. Wang and Y. Lv, *Ceram. Int.*, 2023, **49**, 13355–13362.

159 X. Tang, Z. Hu, Z. Wang, J. Chen, X. Mu, G. Song, P. Sun, Z. Wen, J. Hao, S. Cong and Z. Zhao, *eScience*, 2022, **2**, 632–638.

160 Y. Zhang, B. Xu, B. Huang, T. He, F. Meng, W. Tian, Y. Zhu, J. Wu, H. Wang, H. Li and J. Chen, *ACS Energy Lett.*, 2024, **9**, 4162–4171.

161 Y. Zhao, Q. Liu, Y. Wang, H. Liu, M. Lv, P. Cheng, Y. Fu, J. Li and D. He, *Cell Rep. Phys. Sci.*, 2022, **3**, 101100.

162 J. Koo, V. Amoli, S. Y. Kim, C. Lee, J. Kim, S.-M. Park, J. Kim, J. M. Ahn, K. J. Jung and D. H. Kim, *Nano Energy*, 2020, **78**, 105199.

163 V.-T. Nguyen, B. K. Min, S. K. Kim, Y. Yi and C.-G. Choi, *J. Mater. Chem. C*, 2021, **9**, 3183–3192.

164 Y. Wang, Z. Meng, H. Chen, T. Li, D. Zheng, Q. Xu, H. Wang, X. Y. Liu and W. Guo, *J. Mater. Chem. C*, 2019, **7**, 1966–1973.

165 G. Cai, P. Darmawan, M. Cui, J. Wang, J. Chen, S. Magdassi and P. S. Lee, *Adv. Energy Mater.*, 2016, **6**, 1501882.

166 R. Li, X. Ma, J. Li, J. Cao, H. Gao, T. Li, X. Zhang, L. Wang, Q. Zhang, G. Wang, C. Hou, Y. Li, T. Palacios, Y. Lin, H. Wang and X. Ling, *Nat. Commun.*, 2021, **12**, 1587.

167 W. C. Poh, A. L. S. Eh, W. Wu, X. Guo and P. S. Lee, *Adv. Mater.*, 2022, **34**, 2206952.

168 K. Li, Y. Shao, H. Yan, Z. Lu, K. J. Griffith, J. Yan, G. Wang, H. Fan, J. Lu, W. Huang, B. Bao, X. Liu, C. Hou, Q. Zhang, Y. Li, J. Yu and H. Wang, *Nat. Commun.*, 2018, **9**, 4798.

169 Y. Ling, H. Fan, K. Wang, Z. Lu, L. Wang, C. Hou, Q. Zhang, Y. Li, K. Li and H. Wang, *Small*, 2022, **18**, 2107778.

170 C. Li, M. Zhen, K. Wang, L. Liu, W. Zhang, Y. Wang, X. Fan, W. Hou and J. Xiong, *ACS Appl. Mater. Interfaces*, 2023, **15**, 40772–40780.

171 Z. Yu, G. Cai, X. Liu and D. Tang, *Anal. Chem.*, 2021, **93**, 2916–2925.